Source details

AIP Conference Proceedings

Years currently covered by Scopus: from 1973 to 1978, from 1983 to 1984, 1993, from 2000 to 2001, from 2003 to 2024

ISSN: 0094-243X E-ISSN: 1551-7616

Subject area: Physics and Astronomy: General Physics and Astronomy

Source type: Conference Proceeding

View all documents > | Set document alert | Save to source list

CiteScore 2023
0.5

SJR 2023
0.152

SNIP 2023
0.291

CiteScore | CiteScore rank & trend | Scopus content coverage

CiteScore 2023

$$0.5 = \frac{28{,}862 \text{ Citations } 2020 - 2023}{57{,}814 \text{ Documents } 2020 - 2023}$$

Calculated on 05 May, 2024

CiteScoreTracker 2024

$$0.4 = \frac{20{,}552 \text{ Citations to date}}{56{,}789 \text{ Documents to date}}$$

Last updated on 05 June, 2024 • Updated monthly

CiteScore rank 2023

Category	Rank	Percentile
Physics and Astronomy └ General Physics and Astronomy	#225/243	7th

View CiteScore methodology > | CiteScore FAQ > | Add CiteScore to your site

About Scopus

What is Scopus

Content coverage

Scopus blog

Scopus API

Privacy matters

Language

日本語版を表示する

查看简体中文版本

查看繁體中文版本

Просмотр версии на русском языке

Customer Service

Help

Tutorials

Contact us

AIP Conference Proceedings

COUNTRY	SUBJECT AREA AND CATEGORY	PUBLISHER	H-INDEX
United States Universities and research institutions in United States Media Ranking in United States	Physics and Astronomy Physics and Astronomy (miscellaneous)	American Institute of Physics	83

PUBLICATION TYPE	ISSN	COVERAGE	INFORMATION
Conferences and Proceedings	0094243X, 15517616	1973-1978, 1983-1984, 1993, 2000-2001, 2003-2023	Homepage How to publish in this journal confproc@aip.org

SCOPE

Today, AIP Conference Proceedings contain over 100,000 articles published in 1700+ proceedings and is growing by 100 volumes every year. This substantial body of scientific literature is testament to our 40-year history as a world-class publishing partner, recognized internationally and trusted by conference organizers worldwide. Whether you are planning a small specialist workshop or organizing the largest international conference, contact us, or read these testimonials, to find out why so many organizers publish with AIP Conference Proceedings.

Join the conversation about this journal

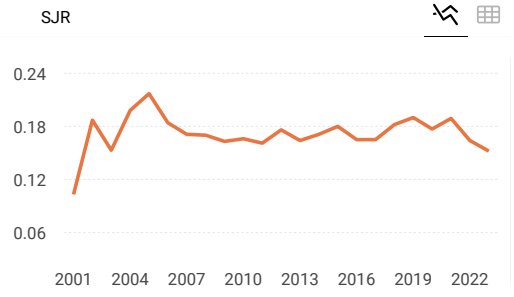

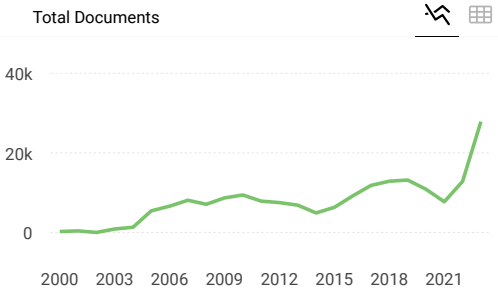

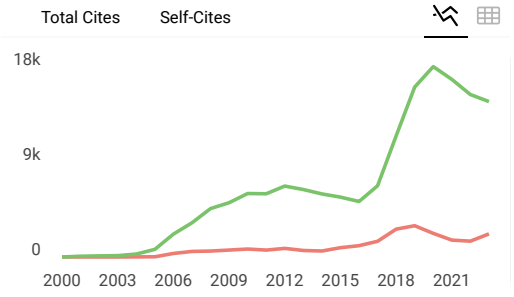

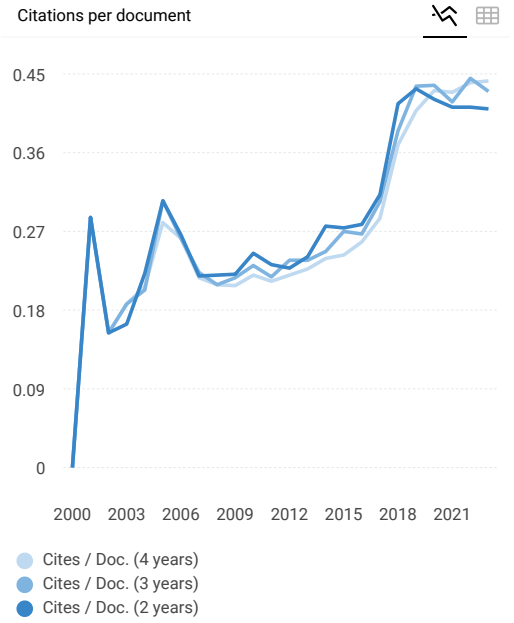

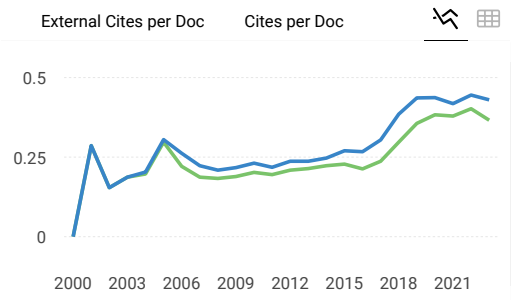

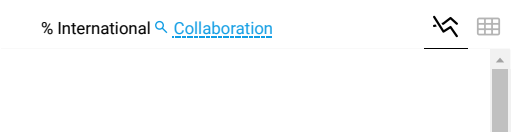

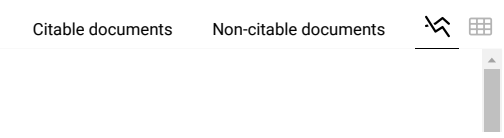

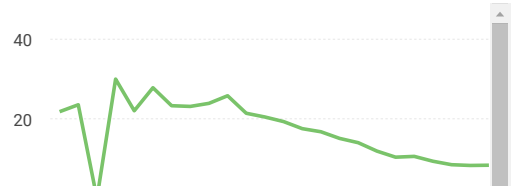

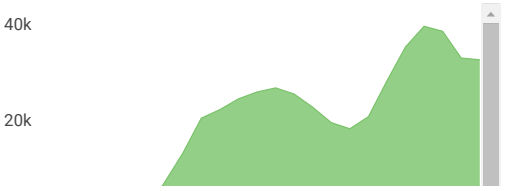

Cited documents Uncited documents

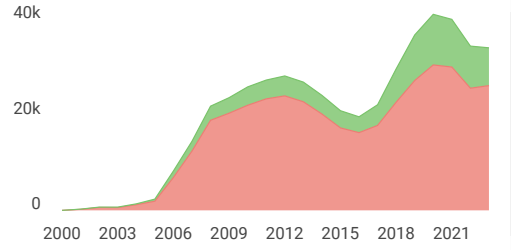

% Female Authors

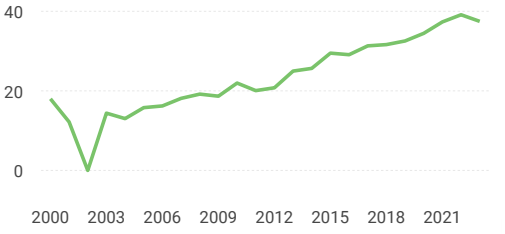

Documents cited by public policy (Overton)

Documents related to SDGs (UN)

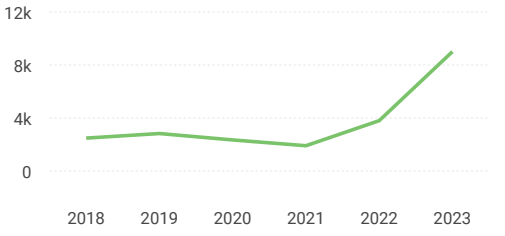

← Show this widget in your own website

Just copy the code below and paste within your html code:

<a href="https://www.scimag

SCImago Graphica

Explore, visually communicate and make sense of data with our **new data visualization tool**.

Metrics based on Scopus® data as of March 2024

D **Dr. Arun Raja R.D.** 1 month ago

AIP CONFERENCE PROCEEDINGS has not been given a quartile rank. What could be it's possibility to be discontinued from Scopus in the recent future? How do we know it?

reply

SCImago Team

Melanie Ortiz 1 month ago

Dear Arun,
Thank you for contacting us. Please see comments below.
Best regards, SCImago Team

Y **Yazeed Alzahrani** 4 months ago

AIP Conference Proceedings

AIP Publishing

Volume 3074

The 7th International Conference on Science and Applied Science (ICSAS 2022)

Surakarta, Indonesia • 21 October 2022

Editors • Budi Purnama, Dewanta Arya Nugraha and A. Suparmi

Available Online: pubs.aip.org/aip/acp

Committees

Advisory Board

1. Assoc. Prof. Mohsen M. Farahat, Central Metallurgical Research and Development Institute, Cairo, Cairo, Egypt
2. Prof. M. Aziz, Tokyo University, Japan
3. Prof. Madya Ts. Dr. Mohd Khairul Bin Ahmad, Universiti Tun Hussein Onn Malaysia
4. Hendri Widiyandari, Universitas Sebelas Maret
5. Ari Handono Ramelan, Universitas Sebelas Maret, Indonesia
6. Cari, Universitas Sebelas Maret, Indonesia
7. Harjana, Universitas Sebelas Maret, Indonesia
8. Suparmi, Universitas Sebelas Maret, Indonesia

Chairman

Budi Purnama, Universitas Sebelas Maret, Indonesia

Organizing Committee

1. Agus Supriyanto, Universitas Sebelas Maret, Indonesia
2. Ahmad Marzuki, Universitas Sebelas Maret, Indonesia
3. Artono Dwijo Sutomo, Universitas Sebelas Maret, Indonesia
4. Budi Legowo, Universitas Sebelas Maret, Indonesia
5. Dewanta Arya Nugraha, Universitas Sebelas Maret, Indonesia
6. Fahru Nurosyid, Universitas Sebelas Maret, Indonesia
7. Fuad Anwar, Universitas Sebelas Maret, Indonesia
8. Hendri Widyandari, Universitas Sebelas Maret, Indonesia
9. Iwan Yahya, Universitas Sebelas Maret, Indonesia
10. Khairuddin, Universitas Sebelas Maret, Indonesia
11. Kusumandari, Universitas Sebelas Maret, Indonesia
12. Mohtar Yunianto, Universitas Sebelas Maret, Indonesia
13. Nuryani, Universitas Sebelas Maret, Indonesia
14. Risa Suryana, Universitas Sebelas Maret, Indonesia
15. Utari, Universitas Sebelas Maret, Indonesia
16. Yofentina Iriani, Universitas Sebelas Maret, Indonesia

Organizer

Physics Department, Universitas Sebelas Maret, | Faculty of Mathematics and Natural Sciences, Indonesia

The 7th International Conference on Science and Applied Science (ICSAS 2022)
AIP Conf. Proc. 3074, 010002-1–010002-1; https://doi.org/10.1063/12.0026243
Published under an exclusive license by AIP Publishing. 978-0-7354-4979-4/$30.00

Preface: The 7th International Conference on Science and Applied Science (ICSAS 2022)

The 7th International Conference on Science and Applied Science (ICSAS 2022) was the sixth conference which was organized by the Physics Department, Universitas Sebelas Maret. On this occasion, the ICSAS 2022 was held virtually on 31 October, 2022, due to the COVID-19 pandemic. The ICSAS 2022 conference is aimed to bring together scholars, leading researchers, and experts from diverse backgrounds and application areas in science. Special emphasis is placed on promoting interaction between the science theoretical, experimental, and other topics related to physics.

In ICSAS 2022, there are 8 parallel sessions and four keynote speakers. The keynote speakers are Assoc. Prof. Mohsen M. Farahat from Central Metallurgical Research and Development Institute, Cairo, Cairo, Egypt; Prof. M. Aziz from Tokyo University, Japan; Prof. Madya Ts. Dr. Mohd Khairul Bin Ahmad from Universiti Tun Hussein Onn Malaysia, and Dr. Eng. Hendri Widiyandari from Universitas Sebelas Maret. While for the conference participants, there is 131 participant which was submitted abstract via the conference system. Then, the 112 full papers have been submitted from the participant, and after the reviewed process, 83 papers have been presented in the ICSAS 2022. And then for the final decision, 49 papers published in AIP Conference Proceedings.

We would like to thank all of the participants attending this conference and also to the committee for their contribution to this high-level conference and its overall success. We also would like to thank the reviewers for their positive contribution to maintain the quality of the articles presented at this conference.

The 7th International Conference on Science and Applied Science (ICSAS 2022)
AIP Conf. Proc. 3074, 010001-1–010001-1; https://doi.org/10.1063/12.0025593
Published under an exclusive license by AIP Publishing. 978-0-7354-4979-4/$30.00

Issues

Select Decade 2020

Select Year 2024

Issue 11 June - Volume 3074, Issue 1

PRELIMINARY

Preface: The 7th International Conference on Science and Applied Science (ICSAS 2022)

AIP Conf. Proc. 3074, 010001 (2024) https://doi.org/10.1063/12.0025593

View article | PDF

Committees: The 7th International Conference on Science and Applied Science (ICSAS 2022)

AIP Conf. Proc. 3074, 010002 (2024) https://doi.org/10.1063/12.0026243

View article | PDF

APPLIED SCIENCE

Numerical study on mechanical properties of cubic porous bone scaffold: Effect of unit cell type

Rochmad Winarso; Rifky Ismail; P. W. Anggoro; J. Jamari; A. P. Bayuseno

AIP Conf. Proc. 3074, 020001 (2024) https://doi.org/10.1063/5.0211261

Abstract | View article | PDF

Immunostick development for Bovine Brucellosis rapid tests in the field

Didik T. Subekti; M. Ibrahim Desem; Susan M. Noor

AIP Conf. Proc. 3074, 020002 (2024) https://doi.org/10.1063/5.0211270

Abstract | View article | PDF

Image segmentation based on active contour in chest X-ray image

Sri Oktamuliani; Yoshifumi Saijo

AIP Conf. Proc. 3074, 020003 (2024) https://doi.org/10.1063/5.0211293

Abstract | View article | PDF

The analysis of adsorption capacity in heavy metal ions by using activated carbon from sago waste

Octolia Togibasa; Khaeriah Dahlan; Yane Oktovina Ansanay; Martina Bunga; Daniel Napitupulu; Tatang Sutarman; Piter Wilson Wafumilena; Beatrix Yuliana Nukuboy

AIP Conf. Proc. 3074, 020004 (2024) https://doi.org/10.1063/5.0211265

Abstract | View article | PDF

The utilization of guava leaves extract (Psidium Guajava L.) to reduce the levels of chrome and nickel heavy metals by atomic absorption spectrophotometry

Nur Hidayati; Mardiyono

AIP Conf. Proc. 3074, 020005 (2024) https://doi.org/10.1063/5.0213711

Abstract | View article | PDF

Fourth and fifth-order Runge-Kutta methods for solving a susceptible-exposed-infected-recovered mathematical model of the spread of COVID-19

Dewi Isabella Palma; Sudi Mungkasi

AIP Conf. Proc. 3074, 020006 (2024) https://doi.org/10.1063/5.0211279

Abstract | View article | PDF

Study the effect of gamma-irradiation on the physical properties of Chitosan powder with the presence of water

Dien Puji Rahayu; Ade Lestari Yunus; Muhammad Yasin Yunus; Farah Nurlidar; Bina Lohita Sari; Reni Lestari; Reni Rosspertiwi

AIP Conf. Proc. 3074, 020007 (2024) https://doi.org/10.1063/5.0211274

Abstract | View article | PDF

Co-dynamics model of the spread of malaria and COVID-19 with numerical solutions using the third-orderand the fourth-order Runge-Kutta methods

Fransiska Intan Rosari; Sudi Mungkasi

AIP Conf. Proc. 3074, 020008 (2024) https://doi.org/10.1063/5.0212225

Abstract | View article | PDF

Prediction of daily solar radiation from weather data using deep learning in the Semarang area

Herliyani Hasanah; Wiji Lestari; Rudi Susanto

AIP Conf. Proc. 3074, 020009 (2024) https://doi.org/10.1063/5.0211352

Abstract | View article | PDF

Calculation of two dimensional photonic bandgap using the Plane Wave Expansion (PWE) method

Ariska Fela Fernanda; Yulianto Agung Rezeki; Anif Jamaluddin; Sri Budiawanti; Lita Rahmasari

AIP Conf. Proc. 3074, 020010 (2024) https://doi.org/10.1063/5.0211278

Abstract | View article | PDF

Enhancing biogas production of Tofu wastewater by co-digestion

Irene A. A. Suwandhi; Sajidan; Arief Budiman; M. Masykuri

AIP Conf. Proc. 3074, 020011 (2024) https://doi.org/10.1063/5.0211284

Abstract | View article | PDF

Managing take-back decisions for a manufacturer and two retailers in the presence of refurbishing

Yahya Putra Pradana; Nughthoh Arfawi Kurdhi; Cucuk Nur Rosyidi

AIP Conf. Proc. 3074, 020012 (2024) https://doi.org/10.1063/5.0211575

Abstract View article PDF

The impact of third-party-oriented refurbishing on new product quality choice for the original equipment manufacturers

Agista Ayuningtyas; Nughthoh Arfawi Kurdhi; Dewi Retno Sari Saputro

AIP Conf. Proc. 3074, 020013 (2024) https://doi.org/10.1063/5.0211574

Abstract View article PDF

The impact of differentiated roof policies on marketing refurbished products

Y. Khennisa Saputri; Nughthoh Arfawi Kurdhi

AIP Conf. Proc. 3074, 020014 (2024) https://doi.org/10.1063/5.0211577

Abstract View article PDF

Samin river flood simulation by using flood mapping model in Sukoharjo regency

Yohana Baptista Nidia Putri Irwani; Cahyono Ikhsan; Ary Setyawan

AIP Conf. Proc. 3074, 020015 (2024) https://doi.org/10.1063/5.0211553

Abstract View article PDF

Mechanical and thermal buckling analysis of functionally graded material (FGM) plate using triangular element

Imam Jauhari Maknun; Bismi Annisa

AIP Conf. Proc. 3074, 020016 (2024) https://doi.org/10.1063/5.0211563

Abstract View article PDF

BIOLOGICAL PHYSICS

The comparative study between single origin tea and herbal tea blends in different brewed-style: Antioxidant assay

Yoga Dwi Jatmiko; Siti Nur Arifah; Mochammad Fitri Atho'illah; Muhaimin Rifa'i

AIP Conf. Proc. 3074, 030001 (2024) https://doi.org/10.1063/5.0211369

Abstract View article PDF

CHEMICAL ENGINEERING

The utilization of sea-salt as a main material for the preparation of sodium ion battery cathode material

Cornelius Satria Yudha; Meidiana Arinawati; Anjas Prasetya Hutama; Enni Apriliyani

AIP Conf. Proc. 3074, 040001 (2024) https://doi.org/10.1063/5.0211282

Abstract View article PDF

Effect of microwave power and extraction time on the yield of highly-valuable vegetable oil and microstructure during microwave-assisted extraction of roselle seeds

Andri Cahyo Kumoro; Diah Susetyo Retnowati; Amanah Mutiarini

AIP Conf. Proc. 3074, 040002 (2024) https://doi.org/10.1063/5.0211289

Abstract View article PDF

A natural dye from agricultural waste of *Nypa fruticans* husk

Firman Asto Putro; Esa Nur Shohih; Paryanto Paryanto; Cornelius Satria Yudha

AIP Conf. Proc. 3074, 040003 (2024) https://doi.org/10.1063/5.0211286

Abstract View article PDF

Optimization of Syngas via tar reduction on empty palm fruit bunch (EFB) bubbling fluidized bed gasification using bentonite

Prima Zuldian; Nurdiah Rahmawati; Astri Pertiwi; Tyas Puspita Rini; Muhammad Arief Yamin; Ardian Salsa Rusmana; Edwin Permana; Erlan Rosyadi; Reiji Noda

AIP Conf. Proc. 3074, 040004 (2024) https://doi.org/10.1063/5.0211358

Abstract View article PDF

Optimization of substrate concentration and inoculum concentration from banana peel on the production of L-lactic acid using *Lactobacillus plantarum* strain FNCC 0020

Abdullah; Dyah Hesti Wardhani; Yufrida Amalia

AIP Conf. Proc. 3074, 040005 (2024) https://doi.org/10.1063/5.0213555

Abstract View article PDF

Syngas production using biomass gasification of downdraft and bubbling fluidized bed

Erlan Rosyadi; Prima Zuldian; Nurdiah Rahmawati; Astri Pertiwi; Tyas Puspita Rini; Ali Nurdin Hidayat; Ardian Salsa Rusmana; M. Arief Yamin; Edwin Permana

AIP Conf. Proc. 3074, 040006 (2024) https://doi.org/10.1063/5.0211453

Abstract View article PDF

Production of pyrolysis active carbon based on tuna head bone waste for supercapacitor applications

Mey Prihandani Wulandari; Rois Fatoni; Tri Widayatno

AIP Conf. Proc. 3074, 040007 (2024) https://doi.org/10.1063/5.0211290

Abstract View article PDF

CHEMISTRY

Acute toxicity test of ethanol extract of gamma irradiated *Vitex trifolia* L. leaves

Susanto; Ermin Katrin Winarno; Hendig Winarno

AIP Conf. Proc. 3074, 050001 (2024) https://doi.org/10.1063/5.0211321

Abstract View article PDF

Acute toxicity test in DDY mice of ethanolic extract of irradiated *Clinacanthus nutans* Lindau leaves

Ermin K. Winarno; Susanto; Hendig Winarno

AIP Conf. Proc. 3074, 050002 (2024) https://doi.org/10.1063/5.0211300

Abstract View article PDF

Simple oxidation method for iodination of Pyrimethamine

Maula Eka Sriyani; Eva Maria Widyasari; Fifi Lifia Yulianti; Zico Daniel Despen Sihombing; Clara Elisa; Iim Halimah; M. Basit Febrian; Teguh Hafidz Ambar Wibawa; Yanuar Setiadi

AIP Conf. Proc. 3074, 050003 (2024) https://doi.org/10.1063/5.0211264

Abstract View article PDF

Studies on efficient removal Cu (II) using magnetite/titania/ZAA nanocomposite

Sri Wahyuni; Ahmad Taufiq; Sumari; Muhammad Rusdi; S. T. Ulfawanti Intan Subadra; Trio Erik Setyawan

AIP Conf. Proc. 3074, 050004 (2024) https://doi.org/10.1063/5.0211756

Abstract View article PDF

MATERIALS ENGINEERING

Gamma irradiation's effect on the performance of ultra high molecular weight polyethylene/hydroxyapatite composite

Farah Nurlidar; Aditya Imam Saputra; Rika Heryani; Nani Suryani; Ade Lestari Yunus; Dien Puji Rahayu; Oktaviani Oktaviani

AIP Conf. Proc. 3074, 060001 (2024) https://doi.org/10.1063/5.0211267

Abstract View article PDF

The effect of granular palm shell activated carbon to reduce CO, HC, and noise on motorcycle Emissions

Maria Roosa Srah Darmanijati; Pranoto; Ari Handono Ramelan; Inayati

AIP Conf. Proc. 3074, 060002 (2024) https://doi.org/10.1063/5.0212711

Abstract View article PDF

Characteristics of water scavenge ejector pump in boeing 700NG

Indreswari Suroso

AIP Conf. Proc. 3074, 060003 (2024) https://doi.org/10.1063/5.0216409

Abstract View article PDF

Analysis of gambier dye as sensitizer to make a significant efficiency improvement

D. G. Saputri; M. K. Ahmad; A. Supriyanto; A. B. Faridahb

AIP Conf. Proc. 3074, 060004 (2024) https://doi.org/10.1063/5.0215053

Abstract View article PDF

PHYSICS

Simple model of sea level peak potentially trigger coastal flood on north coast of Java

Thomas Djamaluddin; Andi Sitti Mariyam; Widodo Setiyo Pranowo; Arif Aditiya; Lesi Mareta; Andi Pengerang Hasanuddin; Ruli Dwi Susanti; Iyus Edi Rusnadi

AIP Conf. Proc. 3074, 070001 (2024) https://doi.org/10.1063/5.0211328

Abstract View article PDF

Optical properties of opal films with graded thickness

Mulda Muldarisnur; Muhammad Engki Saputra; Dahyunir Dahlan

AIP Conf. Proc. 3074, 070002 (2024) https://doi.org/10.1063/5.0211305

Abstract View article PDF

Zodiacal light and astronomical twilight measurement at Timau Nasional Observatory site

Ismail Fahmi; Thomas Djamaluddin; Ahmad Izzuddin; M. Basthoni; Hendro Setyanto; Zam Zam Kusumaatmaja; Ahmad Zulfi Aufar

AIP Conf. Proc. 3074, 070003 (2024) https://doi.org/10.1063/5.0211329

Abstract View article PDF

Development of polyvinyl chloride-methyl yellow film as a dosimeter for gamma-irradiation

Muhamad Yasin Yunus; Farah Nurlidar; Santoso Soekirno

AIP Conf. Proc. 3074, 070004 (2024) https://doi.org/10.1063/5.0211503

Abstract View article PDF

Simulation of gamma radiation interaction of Co-60 with Tungsten, lead, and Bismuth collimator materials using MCNPX

Mukhtar Effendi; Durrotus Sarofina; Wihantoro; Aris Haryadi

AIP Conf. Proc. 3074, 070005 (2024) https://doi.org/10.1063/5.0211283

Abstract View article PDF

Study of the non-relativistic energy spectra of hyperbolic function position dependent mass with Modified Hyperbolic Pöschl Teller potential under AB force

A. Suparmi; S. Maria; C. Cari; S. Faniandari

AIP Conf. Proc. 3074, 070006 (2024) https://doi.org/10.1063/5.0211727

Abstract View article PDF

Analysis of energy eigen values and wave functions of Schrodinger equation with trigonometric function dependent mass for Symmetric Poschl-Teller potential using hypergeometric method

S. Maria; A. Suparmi; C. Cari; S. Faniandari

AIP Conf. Proc. 3074, 070007 (2024) https://doi.org/10.1063/5.0211266

Abstract View article PDF

Gamma radiation shielding properties of TiO_2-doped TeO_2-ZnO-PbO glasses studied using Phy-X lab software

Ahmad Marzuki; Devara Ega Fausta; Agus Tri Purnomo; Nurulhannan Hannani Yannaf; Hafsah Dwi Istiqomah; Retno Willy Astuti

AIP Conf. Proc. 3074, 070008 (2024) https://doi.org/10.1063/5.0211607

Abstract | View article | PDF

Green synthesis and characterization of zinc oxide (ZnO) nanoparticles using Syzygium polyanthum (Wight) Walp. aqueous leaf extract and their application in Al/Mg/KNO_3 pyrotechnics

Evie Lestariana; Yoki Yulizar; Heru Supriyatno

AIP Conf. Proc. 3074, 070009 (2024) https://doi.org/10.1063/5.0216780

Abstract | View article | PDF

Synthesis of amorphous silica (SiO_2) from natural sand minerals using the precipitation method

Siswanto; Adri Supardi; Alifa Nurhaeni

AIP Conf. Proc. 3074, 070010 (2024) https://doi.org/10.1063/5.0211285

Abstract | View article | PDF

Analysis of maximum output power value between organic semiconductors and inorganic semiconductors for thermoelectric modules

M. Reza Ghifari; Iim Fatimah

AIP Conf. Proc. 3074, 070011 (2024) https://doi.org/10.1063/5.0212292

Abstract | View article | PDF

The effect of ozone concentration on degradation of methylene blue using dielectric barrier discharge plasma

Ahmad Qusnudin; K. Kusumandari; Teguh Endah Saraswati

AIP Conf. Proc. 3074, 070012 (2024) https://doi.org/10.1063/5.0212916

Abstract | View article | PDF

Fabrication of HAp/Zn-ferrite nanocomposite for drug delivery application

Fauziyatul Iffah; Ahmad Taufiq; Herlin Pujiarti; Nasikhudin; S. T. Ulfawanti Intan Subadra; Arif Hidayat; Markus Diantoro

AIP Conf. Proc. 3074, 070013 (2024) https://doi.org/10.1063/5.0211757

Abstract | View article | PDF

Synthesis and characterization of silver/Ti-ferrite nanocomposite for drug delivery agent

Illa Aminatul Azizah; Ahmad Taufiq; Joko Utomo; Sunaryono; Arif Hidayat; Nandang Mufti; S. T. Ulfawanti Intan Subadra

AIP Conf. Proc. 3074, 070014 (2024) https://doi.org/10.1063/5.0211758

Abstract | View article | PDF

Comparison of CT number and electron density in 3D printing materials for phantom applications

M. Yunianto; S. Yani; F. Anwar; A. Suparmi; C. Cari; Sarwidi; T. D. Ardyanto

AIP Conf. Proc. 3074, 070015 (2024) https://doi.org/10.1063/5.0211295

Abstract View article PDF

Effect of pumice particle treatment on flexural properties of GFRP composite

Alfiananda Dwiki Arioseno; Kuncoro Diharjo; Dody Ariawan; Andri Rakhman

AIP Conf. Proc. 3074, 070016 (2024) https://doi.org/10.1063/5.0216894

Abstract View article PDF

RESEARCH ARTICLE | JUNE 11 2024

Co-dynamics model of the spread of malaria and COVID-19 with numerical solutions using the third-orderand the fourth-order Runge-Kutta methods

Fransiska Intan Rosari ✉; Sudi Mungkasi

AIP Conf. Proc. 3074, 020008 (2024)
https://doi.org/10.1063/5.0212225

Co-dynamics Model of the Spread of Malaria and COVID-19 with Numerical Solutions using the Third-Order and the Fourth-Order Runge-Kutta Methods

Fransiska Intan Rosari[1, a)] and Sudi Mungkasi[2, b)]

[1]*Department of Mathematics Education, FKIP, Sanata Dharma University, Yogyakarta, Indonesia*
[2]*Department of Mathematics, FST, Sanata Dharma University, Yogyakarta, Indonesia*

[a)]Corresponding author: fransiskaintanrosa07@gmail.com
[b)]sudi@usd.ac.id

Abstract. We describe an existing co-dynamics model of the spread of malaria and COVID-19. Mathematical model can be used to find strategies to control the spread of malaria and COVID-19, so that their spread can be minimised in a population. The mathematical model we use is of the type of the SEI (Susceptible-Exposed-Infected) model for malaria and COVID-19 co-dynamics. For this model, we have three compartments of the human population and three compartments of the vector population. The compartments are based on S (Susceptible subpopulation), E (Exposed subpopulation), and I (Infected subpopulation). Solutions to this mathematical model can be obtained using numerical methods. We use the third-order and the fourth-order Runge-Kutta methods to solve the co-dynamics model. From our simulation results, both methods perform quite well. The fourth-order Runge-Kutta method theoretically has a higher accuracy than the third-order one. Our simulations in this paper confirm that, when solving the SEI model of the spread of malaria and COVID-19, the fourth-order Runge-Kutta method performs better than the third-order Runge-Kutta method.

INTRODUCTION

Infectious diseases are still a big problem in public health because they are one of the main causes of death in the world including in Indonesia. There are many types of infectious diseases until now that require special treatment; this includes malaria and COVID-19. Although their modes of transmission are distinct, both diseases exhibit similar symptoms like fever, headache, and muscle aches. The impact of the disease is dangerous and will be fatal to humans when someone has been infected with COVID-19 and got malaria or vice versa. Malaria is a disease caused by the bite of a female *Anopheles* mosquito with the genus of parasites *Plasmodium*, where the parasite enters and settles in the human liver organs, then infects red blood cells [1]. Four parasitic species that cause malaria in humans are *Plasmodium falciparum, P. vivax, P. malariae,* and *P. ovale.* One of the most common causes of malaria and the leading cause of death is the species Plasmodium falciparum. Transmission and spread of malaria are not only through mosquito bites but through organ donors, blood transfusions, the operation of syringes, and infected fetuses from their mothers [2, 3]. The spread of malaria has three factors, namely humans as hosts, the presence of *Plasmodium* in the body of female mosquitoes as agents, and the environment as a place of longing and resting mosquitoes or vectors [4]. Malaria has an incubation period. At the time of the bite, a mosquito infected with the genus *Plasmodium falciparum* requires an incubation period of 9-14 days to cause the disease, while other types of *Plasmodium* require a different incubation period [5]. The causes of spread, the number of malaria cases, the incubation period of malaria, and symptoms due to malaria infection are also explained in several studies [6–9].

Furthermore, a brand-new respiratory illness that began in Wuhan, China, shocked the world at the end of December 2019 [10, 11]. This disease spread to most countries in the world in a short period, so the World Health Organization (WHO) considered this disease a global problem which came to be known as COVID-19 or

The 7th International Conference on Science and Applied Science (ICSAS 2022)
AIP Conf. Proc. 3074, 020008-1–020008-17; https://doi.org/10.1063/5.0212225

Coronavirus disease [12]. COVID-19 is an infectious disease caused by *Severe Acute Respiratory Syndrome Coronavirus* 2 (SARS-CoV-2). Coronavirus causes respiratory tract infections ranging from cold cough, *Middle East Respiratory Syndrome* (MERS), and severe acute respiratory syndrome, called *Severe Acute Respiratory Syndrome* (SARS) [13, 14]. Since March 2, 2020, COVID-19 has spread in Indonesia [15]. Transmission of COVID-19 can occur directly or indirectly through saliva, respiratory tract, and droplets released when an individual infected coughs, sneezes, talks, or sings [16]. When a susceptible individual to the disease encounters an individual infected with COVID-19, the person is not immediately infected with the virus, but becomes exposed to COVID-19 and requires follow-up health checks such as the swab test. There are two possibilities for a person exposed to COVID-19, namely negative or positive to COVID-19. Data on cases of the spread of COVID-19, symptoms due to Coronavirus infection, causes of transmission, and incubation period are also explained in several studies [17–22].

The COVID-19 pandemic has made the government impose mobility restrictions so that it can have an impact on health service programs and malaria control [23]. An individual exposed to or infected with COVID-19 does not rule out the possibility of being exposed to or infected with other diseases such as malaria and vice versa [24]. These two diseases can coexist to affect and worsen human health, as in the case of co-infection, where a previously healthy young man was later diagnosed with COVID-19 and infected with malaria [25, 26]. This case includes the co-dynamics of the spread of the disease, which is increasingly widespread at any time with a fast transmission rate. Therefore, we need a way to control the spread of malaria and COVID-19, one of which is in the field of mathematics by compiling a mathematical model called the epidemic model. Mathematical modeling helps a person to be able to understand and identify the relationship between the spread of malaria and COVID-19 with various epidemiological parameters and predict the rate of spread of malaria and COVID-19 in the future, so that it does not become more widespread.

During the incubation period of malaria and COVID-19, the population into exposed subpopulations. Several studies have discussed and developed a mathematical model for the co-dynamics of the spread of malaria and COVID-19 or other diseases with various models [27–33]. In this study, we chose not to involve the presence of vaccination, so the appropriate mathematical model for the co-dynamics of this epidemic is the SEI model (Susceptible-Exposed-Infected). We solved the co-dynamics of the spread of malaria and COVID-19 by using numerical methods, namely, Runge-Kutta methods. Runge-Kutta methods are numerical methods used to solve initial value problems in linear or nonlinear ordinary differential equations by achieving the accuracy of the Taylor series approach without requiring higher derivative calculations [34, 35]. There are several types of Runge-Kutta methods, namely the first-, second-, third-, fourth-, fifth-, and higher-order Runge-Kutta methods [35]. Thus, we decided to use two types of Runge-Kutta method, namely the third-, and the fourth-order Runge-Kutta methods, to solve the SEI model on the co-dynamics problem of the spread of malaria and COVID-19, because these two methods are quite popular and known to be sufficiently accurate.

EXPERIMENTAL DETAILS

The mathematical model for the co-dynamics of the spread of malaria and COVID-19 is the model developed in [36]. We use two numerical methods to solve the SEI model. Both of them are the third-order and the fourth-order Runge-Kutta method. Then, we use the MATLAB software for numerical calculations.

SEI Model

The spread of malaria in the SEI model has two populations. There are human and mosquito (vector) populations. The human population in the SEI model for co-dynamics of the spread of malaria and COVID-19 is separated into nine groups, namely Susceptible individuals (S_h), Exposed to malaria only (E_m), Exposed to COVID-19 only (E_C), Exposed to malaria and COVID-19 (E_{mc}), Infected individuals with malaria only (I_m), Infected individuals with COVID-19 only (I_c), Infected with malaria and exposed to COVID-19 $\left(I_{mE_c}\right)$, Infected with both malaria and COVID-19 (I_{mc}), as well as Infected with COVID-19 and exposed to malaria $\left(I_{cE_m}\right)$. Meanwhile, the SEI model for vector populations consists of three groups, Susceptible mosquitoes (S_v), Exposed mosquitoes to the malaria parasite (E_v), and Infectious mosquitoes (I_v). In this case, the groups I_m, I_c, I_{mE_c}, and I_{cE_m} of those who have recovered will be Susceptible individuals again, meaning that an individual is to be exposed to or reinfected with malaria and COVID-19. Our study assumes that there is a group's self-protection against COVID-19. Unlike the human population, the SEI model for vector populations already infected

with *Plasmodium* will not recover but will be alive to be infectious mosquitoes or die naturally. Tchoumi et al. [36] have formed a system of non-linear differential equations to model the spread of malaria and COVID-19 as follows

$$\begin{cases} \frac{dS_h}{dt} = \Lambda_h + \omega_m I_m + \omega_c I_c + \omega_{mc} I_{mc} - (\lambda_m + \lambda_c + \mu) S_h, \\ \frac{dE_m}{dt} = \lambda_m S_h - (\lambda_c + \phi_m + \mu) E_m, \\ \frac{dE_c}{dt} = \lambda_c S_h - (\lambda_m + \phi_c + \mu) E_c, \\ \frac{dE_{mc}}{dt} = \lambda_c E_m + \lambda_m E_c - (\phi_{mc} + \mu) E_{mc}, \\ \frac{dI_m}{dt} = \phi_m E_m - (\delta\lambda_c + \omega_m + \mu) I_m, \\ \frac{dI_c}{dt} = \phi_c E_c - (\epsilon\lambda_m + \omega_c + \mu) I_c, \\ \frac{dI_{mE_c}}{dt} = \delta\lambda_c I_m - (\sigma + \mu) I_{mE_c}, \\ \frac{dI_{mc}}{dt} = \sigma I_{mE_c} + \phi_{mc} E_{mc} + \gamma I_{cE_m} - (\omega_{mc} + \mu) I_{mc}, \\ \frac{dI_{cE_m}}{dt} = \epsilon\lambda_m I_c - (\gamma + \mu) I_{cE_m}, \\ \frac{dS_v}{dt} = \Lambda_v - (\lambda_v + \mu_v) S_v, \\ \frac{dE_v}{dt} = \lambda_v S_v - (\phi_v + \mu_v) E_v, \\ \frac{dI_v}{dt} = \phi_v E_v - (\mu_v) I_v, \end{cases} \tag{1}$$

with initial conditions

$$S_h(0) \geq 0, \;\; E_m(0) \geq 0, \;\; E_c(0) \geq 0, \;\; E_{mc}(0) \geq 0, \;\; I_m(0) \geq 0, \\ I_c(0) \geq 0, \;\; I_{mE_c}(0) \geq 0, \;\; I_{mc}(0) \geq 0, \;\; I_{cE_m}(0) \geq 0. \tag{2}$$

Equation system (1) corresponds to the schematic diagram illustrated by Tchoumi et al. [36]
In addition, the process of transmitting malaria in the mosquito (vector) population is shown as compartment diagram for the SEI model's mosquito component figure by Tchoumi et al. [36]

The description of the variables of equation system (1) for human populations (host) and mosquito populations (vector) from the SEI model is listed in Table 1.

TABLE 1. Variables of the SEI model

Variables	Description
Human (host):	
N_h	Total human population
S_h	Susceptible human subpopulation
E_m	Exposed individuals to malaria only
E_c	Exposed individuals to COVID-19 only
E_{mc}	Exposed individuals to malaria and COVID-19
I_m	Infected individuals to malaria only
I_c	Infected individuals to COVID-19 only
I_{mE_c}	Infected individuals with malaria and exposed to COVID-19
I_{mc}	Infected individuals to malaria and COVID-19
I_{cE_m}	Infected individuals with COVID-19 and exposed to malaria
Mosquitoes (vector):	
N_v	Total vector population
S_v	Susceptible mosquito subpopulation
E_v	Exposed mosquitoes to the malaria parasite
I_v	Infected mosquitoes with malaria

TABLE 2. Parameters of the SEI model

Parameters	Description
Human:	
Λ_h	Host population recruitment rate
ϕ_m	Transfer rate from exposed to infectious malaria state
ϕ_c	Transfer rate from exposed to infectious COVID-19 state
ϕ_{mc}	Proportion of individuals transferring to the co-infection I_{mc} class
ω_m	Rate of recovery of the malaria infected individuals
ω_c	Rate of recovery of the COVID-19 infected individuals
ω_{mc}	Rate of recovery of the malaria and COVID-19 infectious individuals
μ	Host population death rate
δ	Enhancement factor of acquiring COVID-19 following malaria infection
ϵ	Enhancement factor of acquiring malaria following COVID-19 infection
σ	Infection rate of COVID-19 of individuals already infected with malaria
γ	Malaria infection rate of individuals already infected with COVID-19
κ	Proportion of individuals employing personal protection
ζ	Efficacy of personal protection
b	Number of female mosquito bites per day
β_m	Malaria transmission probability per mosquito bite
β_c	Transmission probability of COVID-19 per contact
λ_m	Forces of infection from malaria
λ_c	Forces of infection from COVID-19
Mosquitoes:	
Λ_v	Vector recruitment rate
ϕ_m	Transfer rate from exposed to infectious class
μ_v	Vector natural death rate
β_v	Transmission probability in vector from infected humans
λ_v	Forces of infection from a bite of the malaria parasite

Furthermore, the description of the parameters of equation (1) for human populations and mosquito populations (vector) from the SEI model is listed in Table 2.

In solving the SEI model of equation system (1) and both compartment diagrams for the co-dynamics of the spread of malaria and COVID-19, we choose two methods to obtain solutions, namely the third-, and the fourth-order Runge-Kutta methods.

Third-Order Runge-Kutta Method

Consider the initial value problem $dy/dx = f(x, y),\ y(x_0) = x_0$. Triatmodjo [37] wrote the scheme for the third-order Runge-Kutta method as follows

$$y_{i+1} = y_i + \frac{1}{6}(k_1 + 4k_2 + k_3)h, \tag{3}$$

where h is the step size of the free variable and

$$\begin{aligned} k_1 &= f(x_i, y_i), \\ k_2 &= f\left(x_i + \frac{1}{2}h, y_i + \frac{1}{2}k_1 h\right), \\ k_3 &= f(x_i + h, y_i - k_1 h + 2k_2 h). \end{aligned} \tag{4}$$

We take into account the initial value of each subpopulation $S_{h(1)}, E_{m(1)}, E_{c(1)}, E_{mc(1)}, I_{m(1)}, I_{c(1)}, I_{mE_c(1)}, I_{mc(1)}, I_{cE_m(1)}, S_{v(1)}, E_{v(1)}, I_{v(1)}$, and $N_{h(1)}$ from $S_h(0), E_m(0), E_c(0), E_{mc}(0), I_m(0), I_c(0), I_{mE_c}(0), I_{mc}(0), I_{cE_m}(0), S_v(0), E_v(0), I_v(0)$, and $N_h(0)$, respectively, the third-order Runge-Kutta method to solve the SEI model (1) is

$$\begin{aligned}
S_{h(i+1)} &= S_{h(i)} + \frac{1}{6}\left(k_{1S_h} + 4k_{2S_h} + k_{3S_h}\right)h, \\
E_{m(i+1)} &= E_{m(i)} + \frac{1}{6}\left(k_{1E_m} + 4k_{2E_m} + k_{3E_m}\right)h, \\
E_{c(i+1)} &= E_{c(i)} + \frac{1}{6}\left(k_{1E_c} + 4k_{2E_c} + k_{3E_c}\right)h, \\
E_{mc(i+1)} &= E_{mc(i)} + \frac{1}{6}\left(k_{1E_{mc}} + 4k_{2E_{mc}} + k_{3E_{mc}}\right)h, \\
I_{m_{(i+1)}} &= I_{m(i)} + \frac{1}{6}\left(k_{1I_m} + 4k_{2I_m} + k_{3I_m}\right)h, \\
I_{c_{(i+1)}} &= I_{c(i)} + \frac{1}{6}\left(k_{1I_c} + 4k_{2I_c} + k_{3I_c}\right)h, \\
I_{mE_c(i+1)} &= I_{mE_c(i)} + \frac{1}{6}\left(k_{1I_{mE_c}} + 4k_{2I_{mE_c}} + k_{3I_{mE_c}}\right)h, \\
I_{mc(i+1)} &= I_{mc(i)} + \frac{1}{6}\left(k_{1I_{mc}} + 4k_{2I_{mc}} + k_{3I_{mc}}\right)h, \\
I_{cE_m(i+1)} &= I_{cE_m(i)} + \frac{1}{6}\left(k_{1I_{cE_m}} + 4k_{2I_{cE_m}} + k_{3I_{cE_m}}\right)h, \\
S_{v(i+1)} &= S_{v(i)} + \frac{1}{6}\left(k_{1S_v} + 4k_{2S_v} + k_{3S_v}\right)h, \\
E_{v(i+1)} &= E_{v(i)} + \frac{1}{6}\left(k_{1E_v} + 4k_{2E_v} + k_{3E_v}\right)h, \\
I_{v(i+1)} &= I_{v(i)} + \frac{1}{6}\left(k_{1I_v} + 4k_{2I_v} + k_{3I_v}\right)h, \\
N_{h(i+1)} &= S_{h(i+1)} + E_{m(i+1)} + +E_{c(i+1)} + E_{mc(i+1)} + I_{m(i+1)} + I_{c(i+1)} + I_{mE_c(i+1)} + I_{mc(i+1)} + I_{cE_m(i+1)}, \\
\lambda_c &= \beta_c(1 - \kappa\zeta)\frac{\left(I_{c(i+1)} + I_{mc(i+1)} + I_{cE_m(i+1)}\right)}{N_{h(i+1)}}, \\
\lambda_m &= \beta_m b\frac{I_{v(i+1)}}{N_{h(i+1)}}, \\
\lambda_v &= \beta_v b\frac{\left(I_{m(i+1)} + I_{mc(i+1)} + I_{mE_c(i+1)}\right)}{N_{h(i+1)}}.
\end{aligned} \tag{5}$$

Here, h in the time step, i is the iteration index and:

$$
\begin{aligned}
&k_{1S_h} = \Lambda_h + \omega_m I_{m(i)} + \omega_c I_{c(i)} + \omega_{mc} I_{mc(i)} - (\lambda_m + \lambda_c + \mu) S_{h(i)},\\
&k_{1E_m} = \lambda_m S_{h(i)} - (\lambda_c + \phi_m + \mu) E_{m(i)},\\
&k_{1E_c} = \lambda_c S_{h(i)} - (\lambda_m + \phi_c + \mu) E_{c(i)},\\
&k_{1E_{mc}} = \lambda_c E_{m(i)} + \lambda_m E_{c(i)} - (\phi_{mc} + \mu) E_{mc(i)},\\
&k_{1I_m} = \phi_m E_{m(i)} - (\delta\lambda_c + \omega_m + \mu) I_{m(i)},\\
&k_{1I_c} = \phi_c E_{c(i)} - (\epsilon\lambda_m + \omega_c + \mu) I_{c(i)},\\
&k_{1I_{mE_c}} = \delta\lambda_c I_{m(i)} - (\sigma + \mu) I_{mE_c(i)},\\
&k_{1I_{mc}} = \sigma I_{mE_c(i)} + \phi_{mc} E_{mc(i)} + \gamma I_{cE_m(i)} - (\omega_{mc} + \mu) I_{mc(i)},\\
&k_{1I_{cE_m}} = \epsilon\lambda_m I_{c(i)} - (\gamma + \mu) I_{cE_m(i)},\\
&k_{1S_v} = \Lambda_v - (\lambda_v + \mu_v) S_{v(i)},\\
&k_{1E_v} = \lambda_v S_{v(i)} - (\phi_v + \mu_v) E_{v(i)},\\
&k_{1I_v} = \phi_v E_{v(i)} - (\mu_v) I_{v(i)},
\end{aligned}
$$

$$
\begin{aligned}
&k_{2N_h} = S_{h(i)} + \frac{1}{2}k_{1S_h}h + E_{m(i)} + \frac{1}{2}k_{1E_m}h + E_{c(i)} + \frac{1}{2}k_{1E_c}h + E_{mc(i)} + \frac{1}{2}k_{1E_{mc}}h + I_{m(i)} + \frac{1}{2}k_{1I_m}h\\
&\quad + I_{c(i)} + \frac{1}{2}k_{1I_c}h + I_{mE_c(i)} + \frac{1}{2}k_{1I_{mE_c}}h + I_{mc(i)} + \frac{1}{2}k_{1I_{mc}}h + I_{cE_m(i)} + \frac{1}{2}k_{1I_{cE_m}}h,\\
&\lambda_{c2} = \beta_c(1-\kappa\zeta)\frac{\left(I_{c(i)} + \frac{1}{2}k_{1I_c}h + I_{mc(i)} + \frac{1}{2}k_{1I_{mc}}h + I_{cE_m(i)} + \frac{1}{2}k_{1I_{cE_m}}h\right)}{k_{2N_h}},\\
&\lambda_{m2} = \beta_m b\frac{\left(I_{v(i)} + \frac{1}{2}k_{1I_v}h\right)}{k_{2N_h}},\\
&\lambda_{v2} = \beta_v b\frac{\left(I_{m(i)} + \frac{1}{2}k_{1I_m}h + I_{mc(i)} + \frac{1}{2}k_{1I_{mc}}h + I_{mE_c(i)} + \frac{1}{2}k_{1I_{mE_c}}h\right)}{k_{2N_h}},\\
&k_{2S_h} = \Lambda_h + \omega_m\left(I_{m(i)} + \frac{1}{2}k_{1I_m}h\right) + \omega_c\left(I_{c(i)} + \frac{1}{2}k_{1I_c}h\right) + \omega_{mc}\left(I_{mc(i)} + \frac{1}{2}k_{1I_{mc}}h\right) - (\lambda_{m2} + \lambda_{c2} + \mu)\\
&\quad \left(S_{h(i)} + \frac{1}{2}k_{1S_h}h\right),\\
&k_{2E_m} = \lambda_{m2}\left(S_{h(i)} + \frac{1}{2}k_{1S_h}h\right) - (\lambda_{c2} + \phi_m + \mu)\left(E_{m(i)} + \frac{1}{2}k_{1E_m}h\right),\\
&k_{2E_c} = \lambda_{c2}\left(S_{h(i)} + \frac{1}{2}k_{1S_h}h\right) - (\lambda_{m2} + \phi_c + \mu)\left(E_{c(i)} + \frac{1}{2}k_{1E_c}h\right),\\
&k_{2E_{mc}} = \lambda_{c2}\left(E_{m(i)} + \frac{1}{2}k_{1E_m}h\right) + \lambda_{m2}\left(E_{c(i)} + \frac{1}{2}k_{1E_c}h\right) - (\phi_{mc} + \mu)\left(E_{mc(i)} + \frac{1}{2}k_{1E_{mc}}h\right),\\
&k_{2I_m} = \phi_m\left(E_{m(i)} + \frac{1}{2}k_{1E_m}h\right) - (\delta\lambda_{c2} + \omega_m + \mu)\left(I_{m(i)} + \frac{1}{2}k_{1I_m}h\right),\\
&k_{2I_c} = \phi_c\left(E_{c(i)} + \frac{1}{2}k_{1E_c}h\right) - (\epsilon\lambda_{m2} + \omega_c + \mu)\left(I_{c(i)} + \frac{1}{2}k_{1I_c}h\right),\\
&k_{2I_{mE_c}} = \delta\lambda_{c2}\left(I_{m(i)} + \frac{1}{2}k_{1I_m}h\right) - (\sigma + \mu)\left(I_{mE_c(i)} + \frac{1}{2}k_{1I_{mE_c}}h\right),\\
&k_{2I_{mc}} = \sigma\left(I_{mE_c(i)} + \frac{1}{2}k_{1I_{mE_c}}h\right) + \phi_{mc}\left(E_{mc(i)} + \frac{1}{2}k_{1E_{mc}}h\right) + \gamma\left(I_{cE_m(i)} + \frac{1}{2}k_{1I_{cE_m}}h\right) - (\omega_{mc} + \mu)\\
&\quad \left(I_{mc(i)} + \frac{1}{2}k_{1I_{mc}}h\right),\\
&k_{2I_{cE_m}} = \epsilon\lambda_{m2}\left(I_{c(i)} + \frac{1}{2}k_{1I_c}h\right) - (\gamma + \mu)\left(I_{cE_m(i)} + \frac{1}{2}k_{1I_{cE_m}}h\right),\\
&k_{2S_v} = \Lambda_v - (\lambda_{v2} + \mu_v)\left(S_{v(i)} + \frac{1}{2}k_{1S_v}h\right),\\
&k_{2E_v} = \lambda_{v2}\left(S_{v(i)} + \frac{1}{2}k_{1S_v}h\right) - (\phi_v + \mu_v)\left(E_{v(i)} + \frac{1}{2}k_{1E_v}h\right),
\end{aligned}
\tag{6}
$$

$$k_{2I_v} = \phi_v\left(E_{v(i)} + \frac{1}{2}k_{1E_v}h\right) - (\mu_v)\left(I_{v(i)} + \frac{1}{2}k_{1I_v}h\right),$$

$$\begin{aligned}k_{3N_h} &= \left(S_{h(i)} - k_{1S_h}h + 2k_{2S_h}h\right) + \left(E_{m(i)} - k_{1E_m}h + 2k_{2E_m}h\right) + \left(E_{c(i)} - k_{1E_c}h + 2k_{2E_c}h\right)\\ &\quad + \left(E_{mc(i)} - k_{1E_{mc}}h + 2k_{2E_{mc}}h\right) + \left(I_{m(i)} - k_{1I_m}h + 2k_{2I_m}h\right) + \left(I_{c(i)} - k_{1I_c}h + 2k_{2I_c}h\right)\\ &\quad + \left(I_{mE_c(i)} - k_{1I_{mE_c}}h + 2k_{2I_{mE_c}}h\right) + \left(I_{mc(i)} - k_{1I_{mc}}h + 2k_{2I_{mc}}h\right)\\ &\quad + \left(I_{cE_m(i)} - k_{1I_{cE_m}}h + 2k_{2I_{cE_m}}h\right),\end{aligned}$$

$$\lambda_{c3} = \beta_c(1-\kappa\zeta)\frac{\begin{pmatrix}\left(I_{c(i)} - k_{1I_c}h + 2k_{2I_c}h\right) + \left(I_{mc(i)} - k_{1I_{mc}}h + 2k_{2I_{mc}}h\right)\\ + \left(I_{cE_m(i)} - k_{1I_{cE_m}}h + 2k_{2I_{cE_m}}h\right)\end{pmatrix}}{k_{3N_h}},$$

$$\lambda_{m3} = \beta_m b\frac{\left(I_{v(i)} - k_{1I_v}h + 2k_{2I_v}h\right)}{k_{3N_h}},$$

$$\lambda_{v3} = \beta_v b\frac{\begin{pmatrix}\left(I_{m(i)} - k_{1I_m}h + 2k_{2I_m}h\right) + \left(I_{mc(i)} - k_{1I_{mc}}h + 2k_{2I_{mc}}h\right)\\ + \left(I_{mE_c(i)} - k_{1I_{mE_c}}h + 2k_{2I_{mE_c}}h\right)\end{pmatrix}}{k_{3N_h}},$$

$$\begin{aligned}k_{3S_h} &= \Lambda_h + \omega_m\left(I_{m(i)} - k_{1I_m}h + 2k_{2I_m}h\right) + \omega_c\left(I_{c(i)} - k_{1I_c}h + 2k_{2I_c}h\right)\\ &\quad + \omega_{mc}\left(I_{mc(i)} - k_{1I_{mc}}h + 2k_{2I_{mc}}h\right) - (\lambda_{m3} + \lambda_{c3} + \mu)\left(S_{h(i)} - k_{1S_h}h + 2k_{2S_h}h\right),\end{aligned}$$

$$k_{3E_m} = \lambda_{m3}\left(S_{h(i)} - k_{1S_h}h + 2k_{2S_h}h\right) - (\lambda_{c3} + \phi_m + \mu)\left(E_{m(i)} - k_{1E_m}h + 2k_{2E_m}h\right),$$

$$k_{3E_c} = \lambda_{c3}\left(S_{h(i)} - k_{1S_h}h + 2k_{2S_h}h\right) - (\lambda_{m3} + \phi_c + \mu)\left(E_{c(i)} - k_{1E_c}h + 2k_{2E_c}h\right),$$

$$\begin{aligned}k_{3E_{mc}} &= \lambda_{c3}\left(E_{m(i)} - k_{1E_m}h + 2k_{2E_m}h\right) + \lambda_{m3}\left(E_{c(i)} - k_{1E_c}h + 2k_{2E_c}h\right) - (\phi_{mc} + \mu)\\ &\quad \left(E_{mc(i)} - k_{1E_{mc}}h + 2k_{2E_{mc}}h\right),\end{aligned}$$

$$k_{3I_m} = \phi_m\left(E_{m(i)} - k_{1E_m}h + 2k_{2E_m}h\right) - (\delta\lambda_{c3} + \omega_m + \mu)\left(I_{m(i)} - k_{1I_m}h + 2k_{2I_m}h\right),$$

$$k_{3I_c} = \phi_c\left(E_{c(i)} - k_{1E_c}h + 2k_{2E_c}h\right) - (\epsilon\lambda_{m3} + \omega_c + \mu)\left(I_{c(i)} - k_{1I_c}h + 2k_{2I_c}h\right),$$

$$k_{3I_{mE_c}} = \delta\lambda_{c3}\left(I_{m(i)} - k_{1I_m}h + 2k_{2I_m}h\right) - (\sigma + \mu)\left(I_{mE_c(i)} - k_{1I_{mE_c}}h + 2k_{2I_{mE_c}}h\right),$$

$$\begin{aligned}k_{3I_{mc}} &= \sigma\left(I_{mE_c(i)} - k_{1I_{mE_c}}h + 2k_{2I_{mE_c}}h\right) + \phi_{mc}\left(E_{mc(i)} - k_{1E_{mc}}h + 2k_{2E_{mc}}h\right)\\ &\quad + \gamma\left(I_{cE_m(i)} - k_{1I_{cE_m}}h + 2k_{2I_{cE_m}}h\right) - (\omega_{mc} + \mu)\left(I_{mc(i)} - k_{1I_{mc}}h + 2k_{2I_{mc}}h\right),\end{aligned}$$

$$k_{3I_{cE_m}} = \epsilon\lambda_{m3}\left(I_{c(i)} - k_{1I_c}h + 2k_{2I_c}h\right) - (\gamma + \mu)\left(I_{cE_m(i)} - k_{1I_{cE_m}}h + 2k_{2I_{cE_m}}h\right),$$

$$k_{3S_v} = \Lambda_v - (\lambda_{v3} + \mu_v)\left(S_{v(i)} - k_{1S_v}h + 2k_{2S_v}h\right),$$

$$k_{3E_v} = \lambda_{v3}\left(S_{v(i)} - k_{1S_v}h + 2k_{2S_v}h\right) - (\phi_v + \mu_v)\left(E_{v(i)} - k_{1E_v}h + 2k_{2E_v}h\right),$$

$$k_{3I_v} = \phi_v\left(E_{v(i)} - k_{1E_v}h + 2k_{2E_v}h\right) - (\mu_v)\left(I_{v(i)} - k_{1I_v}h + 2k_{2I_v}h\right).$$

Fourth-Order Runge-Kutta Method

The fourth-order Runge-Kutta method is one of the numerical methods for solving differential equations that can be derived from Taylor expansions [38, 39]. This method has a higher order of solution accuracy than the first-, the second-, and the third-order methods [40]. Reconsider the initial value problem $dy/dx = f(x,y)$, $y(x_0) = x_0$, Chapra and Canale [41] wrote down the most commonly used form of the classical fourth-order Runge-Kutta method as follows

$$y_{i+1} = y_i + \frac{1}{6}(k_1 + 2k_2 + 2k_3 + k_4)h, \tag{7}$$

where

$$
\begin{aligned}
k_1 &= f(x_i, y_i),\\
k_2 &= f\left(x_i + \frac{1}{2}h, y_i + \frac{1}{2}k_1 h\right),\\
k_3 &= f\left(x_i + \frac{1}{2}h, y_i + \frac{1}{2}k_2 h\right),\\
k_4 &= f(x_i + h, y_i + k_3 h).
\end{aligned} \tag{8}
$$

Now, we take into account the initial value of each subpopulation $S_{h(1)}$, $E_{m(1)}$, $E_{c(1)}$, $E_{mc(1)}$, $I_{m(1)}$, $I_{c(1)}$, $I_{mE_c(1)}$, $I_{mc(1)}$, $I_{cE_m(1)}$, $S_{v(1)}, E_{v(1)}$, $I_{v(1)}$, and $N_{h(1)}$ from $S_h(0), E_m(0)$, $E_c(0)$, $E_{mc}(0)$, $I_m(0)$, $I_c(0)$, $I_{mE_c}(0)$, $I_{mc}(0)$, $I_{cE_m}(0)$, $S_v(0), E_v(0)$, $I_v(0)$, and $N_h(0)$, respectively, the fourth-order Runge-Kutta method to solve the SEI model (1) is

$$
\begin{aligned}
S_{h(i+1)} &= S_{h(i)} + \frac{1}{6}\left(k_{1S_h} + 2k_{2S_h} + 2k_{3S_h} + k_{4S_h}\right)h,\\
E_{m(i+1)} &= E_{m(i)} + \frac{1}{6}\left(k_{1E_m} + 2k_{2E_m} + 2k_{3E_m} + k_{4E_m}\right)h,\\
E_{c(i+1)} &= E_{c(i)} + \frac{1}{6}\left(k_{1E_c} + 2k_{2E_c} + 2k_{3E_c} + k_{4E_c}\right)h,\\
E_{mc(i+1)} &= E_{mc(i)} + \frac{1}{6}\left(k_{1E_{mc}} + 2k_{2E_{mc}} + 2k_{3E_{mc}} + k_{4E_{mc}}\right)h,\\
I_{m_{(i+1)}} &= I_{m(i)} + \frac{1}{6}\left(k_{1I_m} + 2k_{2I_m} + 2k_{3I_m} + k_{4I_m}\right)h,\\
I_{c_{(i+1)}} &= I_{c(i)} + \frac{1}{6}\left(k_{1I_c} + 2k_{2I_c} + 2k_{3I_c} + k_{4I_c}\right)h,\\
I_{mE_c(i+1)} &= I_{mE_c(i)} + \frac{1}{6}\left(k_{1I_{mE_c}} + 2k_{2I_{mE_c}} + 2k_{3I_{mE_c}} + k_{4I_{mE_c}}\right)h,\\
I_{mc(i+1)} &= I_{mc(i)} + \frac{1}{6}\left(k_{1I_{mc}} + 2k_{2I_{mc}} + 2k_{3I_{mc}} + k_{4I_{mc}}\right)h,\\
I_{cE_m(i+1)} &= I_{cE_m(i)} + \frac{1}{6}\left(k_{1I_{cE_m}} + 2k_{2I_{cE_m}} + 2k_{3I_{cE_m}} + k_{4I_{cE_m}}\right)h,\\
S_{v(i+1)} &= S_{v(i)} + \frac{1}{6}\left(k_{1S_v} + 2k_{2S_v} + 2k_{3S_v} + k_{4S_v}\right)h,\\
E_{v(i+1)} &= E_{v(i)} + \frac{1}{6}\left(k_{1E_v} + 2k_{2E_v} + 2k_{3E_v} + k_{4E_v}\right)h,\\
I_{v(i+1)} &= I_{v(i)} + \frac{1}{6}\left(k_{1I_v} + 2k_{2I_v} + 2k_{3I_v} + k_{4I_v}\right)h,\\
N_{h(i+1)} &= S_{h(i+1)} + E_{m(i+1)} + +E_{c(i+1)} + E_{mc(i+1)} + I_{m(i+1)} + I_{c(i+1)} + I_{mE_c(i+1)} + I_{mc(i+1)} + I_{cE_m(i+1)}\\
\lambda_c &= \beta_c(1-\kappa\zeta)\frac{\left(I_{c(i+1)} + I_{mc(i+1)} + I_{cE_m(i+1)}\right)}{N_{h(i+1)}},\\
\lambda_m &= \beta_m b\frac{I_{v(i+1)}}{N_{h(i+1)}},\\
\lambda_v &= \beta_v b\frac{\left(I_{m(i+1)} + I_{mc(i+1)} + I_{mE_c(i+1)}\right)}{N_{h(i+1)}}.
\end{aligned} \tag{9}
$$

Here, h is the time step, i is the iteration index and:

$$
\begin{aligned}
&k_{1S_h} = \Lambda_h + \omega_m I_{m(i)} + \omega_c I_{c(i)} + \omega_{mc} I_{mc(i)} - (\lambda_m + \lambda_c + \mu)S_{h(i)},\\
&k_{1E_m} = \lambda_m S_{h(i)} - (\lambda_c + \phi_m + \mu)E_{m(i)},\\
&k_{1E_c} = \lambda_c S_{h(i)} - (\lambda_m + \phi_c + \mu)E_{c(i)},\\
&k_{1E_{mc}} = \lambda_c E_{m(i)} + \lambda_m E_{c(i)} - (\phi_{mc} + \mu)E_{mc(i)},\\
&k_{1I_m} = \phi_m E_{m(i)} - (\delta\lambda_c + \omega_m + \mu)I_{m(i)},\\
&k_{1I_c} = \phi_c E_{c(i)} - (\epsilon\lambda_m + \omega_c + \mu)I_{c(i)},\\
&k_{1I_{mE_c}} = \delta\lambda_c I_{m(i)} - (\sigma + \mu)I_{mE_c(i)},\\
&k_{1I_{mc}} = \sigma I_{mE_c(i)} + \phi_{mc} E_{mc(i)} + \gamma I_{cE_m(i)} - (\omega_{mc} + \mu)I_{mc(i)},
\end{aligned} \tag{10}
$$

$$k_{1I_{cE_m}} = \epsilon\lambda_m I_{c(i)} - (\gamma+\mu)I_{cE_m(i)},$$
$$k_{1S_v} = \Lambda_v - (\lambda_v+\mu_v)S_{v(i)},$$
$$k_{1E_v} = \lambda_v S_{v(i)} - (\phi_v+\mu_v)E_{v(i)},$$
$$k_{1I_v} = \phi_v E_{v(i)} - (\mu_v)I_{v(i)},$$

$$k_{2N_h} = S_{h(i)} + \frac{1}{2}k_{1S_h}h + E_{m(i)} + \frac{1}{2}k_{1E_m}h + E_{c(i)} + \frac{1}{2}k_{1E_c}h + E_{mc(i)} + \frac{1}{2}k_{1E_{mc}}h + I_{m(i)} + \frac{1}{2}k_{1I_m}h + I_{c(i)} + \frac{1}{2}k_{1I_c}h + I_{mE_c(i)} + \frac{1}{2}k_{1I_{mE_c}}h + I_{mc(i)} + \frac{1}{2}k_{1I_{mc}}h + I_{cE_m(i)} + \frac{1}{2}k_{1I_{cE_m}}h,$$

$$\lambda_{c2} = \beta_c(1-\kappa\zeta)\frac{\left(I_{c(i)} + \frac{1}{2}k_{1I_c}h + I_{mc(i)} + \frac{1}{2}k_{1I_{mc}}h + I_{cE_m(i)} + \frac{1}{2}k_{1I_{cE_m}}h\right)}{k_{2N_h}},$$

$$\lambda_{m2} = \beta_m b\frac{\left(I_{v(i)} + \frac{1}{2}k_{1I_v}h\right)}{k_{2N_h}},$$

$$\lambda_{v2} = \beta_v b\frac{\left(I_{m(i)} + \frac{1}{2}k_{1I_m}h + I_{mc(i)} + \frac{1}{2}k_{1I_{mc}}h + I_{mE_c(i)} + \frac{1}{2}k_{1I_{mE_c}}h\right)}{k_{2N_h}},$$

$$k_{2S_h} = \Lambda_h + \omega_m\left(I_{m(i)} + \frac{1}{2}k_{1I_m}h\right) + \omega_c\left(I_{c(i)} + \frac{1}{2}k_{1I_c}h\right) + \omega_{mc}\left(I_{mc(i)} + \frac{1}{2}k_{1I_{mc}}h\right) - (\lambda_{m2}+\lambda_{c2}+\mu)\left(S_{h(i)} + \frac{1}{2}k_{1S_h}h\right),$$

$$k_{2E_m} = \lambda_{m2}\left(S_{h(i)} + \frac{1}{2}k_{1S_h}h\right) - (\lambda_{c2}+\phi_m+\mu)\left(E_{m(i)} + \frac{1}{2}k_{1E_m}h\right),$$

$$k_{2E_c} = \lambda_{c2}\left(S_{h(i)} + \frac{1}{2}k_{1S_h}h\right) - (\lambda_{m2}+\phi_c+\mu)\left(E_{c(i)} + \frac{1}{2}k_{1E_c}h\right),$$

$$k_{2E_{mc}} = \lambda_{c2}\left(E_{m(i)} + \frac{1}{2}k_{1E_m}h\right) + \lambda_{m2}\left(E_{c(i)} + \frac{1}{2}k_{1E_c}h\right) - (\phi_{mc}+\mu)\left(E_{mc(i)} + \frac{1}{2}k_{1E_{mc}}h\right),$$

$$k_{2I_m} = \phi_m\left(E_{m(i)} + \frac{1}{2}k_{1E_m}h\right) - (\delta\lambda_{c2}+\omega_m+\mu)\left(I_{m(i)} + \frac{1}{2}k_{1I_m}h\right),$$

$$k_{2I_c} = \phi_c\left(E_{c(i)} + \frac{1}{2}k_{1E_c}h\right) - (\epsilon\lambda_{m2}+\omega_c+\mu)\left(I_{c(i)} + \frac{1}{2}k_{1I_c}h\right),$$

$$k_{2I_{mE_c}} = \delta\lambda_{c2}\left(I_{m(i)} + \frac{1}{2}k_{1I_m}h\right) - (\sigma+\mu)\left(I_{mE_c(i)} + \frac{1}{2}k_{1I_{mE_c}}h\right),$$

$$k_{2I_{mc}} = \sigma\left(I_{mE_c(i)} + \frac{1}{2}k_{1I_{mE_c}}h\right) + \phi_{mc}\left(E_{mc(i)} + \frac{1}{2}k_{1E_{mc}}h\right) + \gamma\left(I_{cE_m(i)} + \frac{1}{2}k_{1I_{cE_m}}h\right) - (\omega_{mc}+\mu)\left(I_{mc(i)} + \frac{1}{2}k_{1I_{mc}}h\right),$$

$$k_{2I_{cE_m}} = \epsilon\lambda_{m2}\left(I_{c(i)} + \frac{1}{2}k_{1I_c}h\right) - (\gamma+\mu)\left(I_{cE_m(i)} + \frac{1}{2}k_{1I_{cE_m}}h\right),$$

$$k_{2S_v} = \Lambda_v - (\lambda_{v2}+\mu_v)\left(S_{v(i)} + \frac{1}{2}k_{1S_v}h\right),$$

$$k_{2E_v} = \lambda_{v2}\left(S_{v(i)} + \frac{1}{2}k_{1S_v}h\right) - (\phi_v+\mu_v)\left(E_{v(i)} + \frac{1}{2}k_{1E_v}h\right),$$

$$k_{2I_v} = \phi_v\left(E_{v(i)} + \frac{1}{2}k_{1E_v}h\right) - (\mu_v)\left(I_{v(i)} + \frac{1}{2}k_{1I_v}h\right),$$

$$k_{3N_h} = S_{h(i)} + \frac{1}{2}k_{2S_h}h + E_{m(i)} + \frac{1}{2}k_{2E_m}h + E_{c(i)} + \frac{1}{2}k_{2E_c}h + E_{mc(i)} + \frac{1}{2}k_{2E_{mc}}h + I_{m(i)} + \frac{1}{2}k_{2I_m}h + I_{c(i)} + \frac{1}{2}k_{2I_c}h + I_{mE_c(i)} + \frac{1}{2}k_{2I_{mE_c}}h + I_{mc(i)} + \frac{1}{2}k_{2I_{mc}}h + I_{cE_m(i)} + \frac{1}{2}k_{2I_{cE_m}}h,$$

$$\lambda_{c3} = \beta_c(1-\kappa\zeta)\frac{\left(I_{c(i)} + \frac{1}{2}k_{2I_c}h + I_{mc(i)} + \frac{1}{2}k_{2I_{mc}}h + I_{cE_m(i)} + \frac{1}{2}k_{2I_{cE_m}}h\right)}{k_{3N_h}},$$

$$\lambda_{m3} = \beta_m b \frac{\left(I_{v(i)} + \frac{1}{2}k_{2I_v}h\right)}{k_{3N_h}},$$

$$\lambda_{v3} = \beta_v b \frac{\left(I_{m(i)} + \frac{1}{2}k_{2I_m}h + I_{mc(i)} + \frac{1}{2}k_{2I_{mc}}h + I_{mE_c(i)} + \frac{1}{2}k_{2I_{mE_c}}h\right)}{k_{3N_h}},$$

$$k_{3S_h} = \Lambda_h + \omega_m\left(I_{m(i)} + \frac{1}{2}k_{2I_m}h\right) + \omega_c\left(I_{c(i)} + \frac{1}{2}k_{2I_c}h\right) + \omega_{mc}\left(I_{mc(i)} + \frac{1}{2}k_{2I_{mc}}h\right) - (\lambda_{m3} + \lambda_{c3} + \mu)\left(S_{h(i)} + \frac{1}{2}k_{2S_h}h\right),$$

$$k_{3E_m} = \lambda_{m3}\left(S_{h(i)} + \frac{1}{2}k_{2S_h}h\right) - (\lambda_{c3} + \phi_m + \mu)\left(E_{m(i)} + \frac{1}{2}k_{2E_m}h\right),$$

$$k_{3E_c} = \lambda_{c3}\left(S_{h(i)} + \frac{1}{2}k_{2S_h}h\right) - (\lambda_{m3} + \phi_c + \mu)\left(E_{c(i)} + \frac{1}{2}k_{2E_c}h\right),$$

$$k_{3E_{mc}} = \lambda_{c3}\left(E_{m(i)} + \frac{1}{2}\ k_{2E_m}h\right) + \lambda_{m3}\left(E_{c(i)} + \frac{1}{2}k_{2E_c}h\right) - (\phi_{mc} + \mu)\left(E_{mc(i)} + \frac{1}{2}k_{2E_{mc}}h\right),$$

$$k_{3I_m} = \phi_m\left(E_{m(i)} + \frac{1}{2}k_{2E_m}h\right) - (\delta\lambda_{c3} + \omega_m + \mu)\left(I_{m(i)} + \frac{1}{2}k_{2I_m}h\right),$$

$$k_{3I_c} = \phi_c\left(E_{c(i)} + \frac{1}{2}k_{2E_c}h\right) - (\epsilon\lambda_{m3} + \omega_c + \mu)\left(I_{c(i)} + \frac{1}{2}k_{2I_c}h\right),$$

$$k_{3I_{mE_c}} = \delta\lambda_{c3}\left(I_{m(i)} + \frac{1}{2}k_{2I_m}h\right) - (\sigma + \mu)\left(I_{mE_c(i)} + \frac{1}{2}k_{2I_{mE_c}}h\right),$$

$$k_{3I_{mc}} = \sigma\left(I_{mE_c(i)} + \frac{1}{2}k_{2I_{mE_c}}h\right) + \phi_{mc}\left(E_{mc(i)} + \frac{1}{2}k_{2E_{mc}}h\right) + \gamma\left(I_{cE_m(i)} + \frac{1}{2}k_{2I_{cE_m}}h\right) - (\omega_{mc} + \mu)\left(I_{mc(i)} + \frac{1}{2}k_{2I_{mc}}h\right),$$

$$k_{3I_{cE_m}} = \epsilon\lambda_{m3}\left(I_{c(i)} + \frac{1}{2}k_{2I_c}h\right) - (\gamma + \mu)\left(I_{cE_m(i)} + \frac{1}{2}k_{2I_{cE_m}}h\right),$$

$$k_{3S_v} = \Lambda_v - (\lambda_{v3} + \mu_v)\left(S_{v(i)} + \frac{1}{2}k_{2S_v}h\right),$$

$$k_{3E_v} = \lambda_{v3}\left(S_{v(i)} + \frac{1}{2}k_{2S_v}h\right) - (\phi_v + \mu_v)\left(E_{v(i)} + \frac{1}{2}k_{2E_v}h\right),$$

$$k_{3I_v} = \phi_v\left(E_{v(i)} + \frac{1}{2}k_{2E_v}h\right) - (\mu_v)\left(I_{v(i)} + \frac{1}{2}k_{2I_v}h\right),$$

$$k_{4N_h} = S_{h(i)} + k_{3S_h}h + E_{m(i)} + k_{3E_m}h + E_{c(i)} + k_{3E_c}h + E_{mc(i)} + k_{3E_{mc}}h + I_{m(i)} + k_{3I_m}h + I_{c(i)} + k_{3I_c}h + I_{mE_c(i)} + k_{3I_{mE_c}}h + I_{mc(i)} + k_{3I_{mc}}h + I_{cE_m(i)} + k_{3I_{cE_m}}h,$$

$$\lambda_{c4} = \beta_c(1 - \kappa\zeta)\frac{\left(I_{c(i)} + k_{3I_c}h + I_{mc(i)} + k_{3I_{mc}}h + I_{cE_m(i)} + k_{3I_{cE_m}}h\right)}{k_{4N_h}},$$

$$\lambda_{m4} = \beta_m b \frac{\left(I_{v(i)} + k_{3I_v}h\right)}{k_{4N_h}},$$

$$\lambda_{v4} = \beta_v b \frac{\left(I_{m(i)} + k_{3I_m}h + I_{mc(i)} + k_{3I_{mc}}h + I_{mE_c(i)} + k_{3I_{mE_c}}h\right)}{k_{4N_h}},$$

$$k_{4S_h} = \Lambda_h + \omega_m\left(I_{m(i)} + k_{3I_m}h\right) + \omega_c\left(I_{c(i)} + k_{3I_c}h\right) + \omega_{mc}\left(I_{mc(i)} + k_{3I_{mc}}h\right) - (\lambda_{m4} + \lambda_{c4} + \mu)\left(S_{h(i)} + k_{3S_h}h\right),$$

$$k_{4E_m} = \lambda_{m4}\left(S_{h(i)} + k_{3S_h}h\right) - (\lambda_{c4} + \phi_m + \mu)\left(E_{m(i)} + k_{3E_m}h\right),$$

$$k_{4E_c} = \lambda_{c4}\left(S_{h(i)} + k_{3S_h}h\right) - (\lambda_{m4} + \phi_c + \mu)\left(E_{c(i)} + k_{3E_c}h\right),$$

$$k_{4E_{mc}} = \lambda_{c4}\left(E_{m(i)} + k_{3E_m}h\right) + \lambda_{m4}\left(E_{c(i)} + k_{3E_c}h\right) - (\phi_{mc} + \mu)\left(E_{mc(i)} + k_{3E_{mc}}h\right),$$

$$k_{4I_m} = \phi_m\left(E_{m(i)} + k_{3E_m}h\right) - (\delta\lambda_{c4} + \omega_m + \mu)\left(I_{m(i)} + k_{3I_m}h\right),$$

$$k_{4I_c} = \phi_c\left(E_{c(i)} + k_{3E_c}h\right) - (\epsilon\lambda_{m4} + \omega_c + \mu)\left(I_{c(i)} + k_{3I_c}h\right),$$

$$k_{4I_{mE_c}} = \delta\lambda_{c4}\left(I_{m(i)} + k_{3I_m}h\right) - (\sigma + \mu)\left(I_{mE_c(i)} + k_{3I_{mE_c}}h\right),$$
$$k_{4I_{mc}} = \sigma\left(I_{mE_c(i)} + k_{3I_{mE_c}}h\right) + \phi_{mc}\left(E_{mc(i)} + k_{3E_{mc}}h\right) + \gamma\left(I_{cE_m(i)} + k_{3I_{cE_m}}h\right) - (\omega_{mc} + \mu)\left(I_{mc(i)} + k_{3I_{mc}}h\right),$$
$$k_{4I_{cE_m}} = \epsilon\lambda_{m4}\left(I_{c(i)} + k_{3I_c}h\right) - (\gamma + \mu)\left(I_{cE_m(i)} + k_{3I_{cE_m}}h\right),$$
$$k_{4S_v} = \Lambda_v - (\lambda_{v4} + \mu_v)\left(S_{v(i)} + k_{3S_v}h\right),$$
$$k_{4E_v} = \lambda_{v4}\left(S_{v(i)} + k_{3S_v}h\right) - (\phi_v + \mu_v)\left(E_{v(i)} + k_{3E_v}h\right),$$
$$k_{4I_v} = \phi_v\left(E_{v(i)} + k_{3E_v}h\right) - (\mu_v)\left(I_{v(i)} + k_{3I_v}h\right).$$

RESULTS AND DISCUSSION

The numerical simulation results and the accuracy of the SEI models of the third-, and fourth-order Runge-Kutta methods are discussed in this section. Simulations are conducted using the MATLAB software and the calculation of the accuracy order using the Microsoft Excel software. Numerical simulations require initial values. Therefore, we use the third-order and fourth-order Runge-Kutta methods to solve equation (1) in the SEI model. The initial values of the variable and its parameters are listed in Table 3 and Table 4.

TABLE 3. Initial Values of Variables of the SEI model

Variables	Values
Human	
$N_{h(1)}$	$S_{h(1)} + E_{m(1)} + +E_{c(1)} + E_{mc(1)} + I_{m(1)} + I_{c(1)} + I_{mE_c(1)} + I_{mc(1)} + I_{cE_m(1)}$
$S_{h(1)}$	2500
$E_{m(1)}$	1
$E_{c(1)}$	1
$E_{mc(1)}$	1
$I_{m(1)}$	10
$I_{c(1)}$	20
$I_{mE_c(1)}$	1
$I_{mc(1)}$	3
$I_{cE_m(1)}$	3
Mosquitoes (vector)	
$N_{v(1)}$	$S_{v(1)} + E_{v(1)} + I_{v(1)}$
$S_{v(1)}$	10000
$E_{v(1)}$	8
$I_{v(1)}$	10

The initial values of λ_c, λ_m, and λ_v are in the form of a predefined formula [36]. It means the three parameters have values that can change following the value of other related variables and the parameters. Wearing health masks, social and physical distance, hydro alcoholic gel, hand washing with soap, gathering intensity, and self-isolation were also included in this study as methods of community personal protection against COVID-19. This condition also brings up the efficacy of personal protection. A factor $(1 - \kappa\zeta)$ is used to represent the effect of personal protection, where $0 < \zeta < 1$ and $0 < \kappa < 1$. During the simulation, we selected initial values $\zeta = 0.5$ and $\kappa = 0.5$, which indicate that 50% of humans apply for personal protection. Then, the initial value of malaria transmission probability per mosquito bite, β_m selected 0.125 on numerical simulations.

TABLE 4. Initial Values of Parameters of the SEI model

Parameters	Values
Human	
Λ_h	$\frac{10000}{59\times365}$
ϕ_m	0.8333
ϕ_c	0.6
ϕ_{mc}	0.333
ω_m	0.25
ω_c	0.3
ω_{mc}	0.025
μ	$\frac{1}{59\times365}$
δ	1.02
ϵ	1.01
σ	0.4
γ	0.0833
κ	0 – 1
ζ	0 – 1
b	4.3 × 0.33
β_m	0.125 – 0.5
β_c	0.4531
λ_c	$\beta_c(1-\kappa\zeta)\frac{\left(I_{c(1)}+I_{mc(1)}+I_{cE_m(1)}\right)}{N_{h(1)}}$
λ_m	$\beta_m b\frac{I_{v(1)}}{N_{h(1)}}$
Mosquitoes	
Λ_v	$\frac{10^4}{21}$
ϕ_m	0.1
μ_v	$\frac{1}{21}$
β_v	0.48
λ_v	$\beta_v b\frac{\left(I_{m(1)}+I_{mc(1)}+I_{mE_c(1)}\right)}{N_{h(1)}}$

Simulation Results of the Third-Order Runge-Kutta Method

The behavior of the co-dynamics of the spread of COVID-19 and malaria using the SEI model and the third-order Runge-Kutta method is depicted in Figure 1. The number of humans susceptible to malaria and COVID-19, namely, S_h, has decreased over time. That is because the number of individuals exposed to malaria only, namely E_m, increased at a certain period. That also happened to individuals exposed to COVID-19 only, namely E_c. However, at the same time, both subpopulations have decreased. The increasing number of individuals exposed to malaria or COVID-19 can open opportunities to influence the increase in the number of individuals infected. Initially, the number of individuals infected with malaria only, namely I_m, and individuals infected with COVID-19 only, namely I_c, decreased and stayed around a certain value at a certain period. Then the number increased over a long period and decreased again. Such behavior also occurs in the number of individuals infected with malaria and exposed to COVID-19, namely I_{mE_c}, and the number of individuals infected with COVID-19 and exposed to malaria, namely I_{cE_m}. These dynamics also occur in individuals exposed to malaria and COVID-19, namely E_{mc}, and individuals infected with malaria and COVID-19, namely I_{mc}, in the span of 0 to 60. Meanwhile, when close to infinity, $S_h(t)$, $E_m(t)$, $E_c(t)$, $E_{mc}(t)$, $I_m(t)$, $I_c(t)$, $I_{mE_c}(t)$, $I_{mc}(t)$, and $I_{cE_m}(t)$ will be constants. The human population will never become extinct.

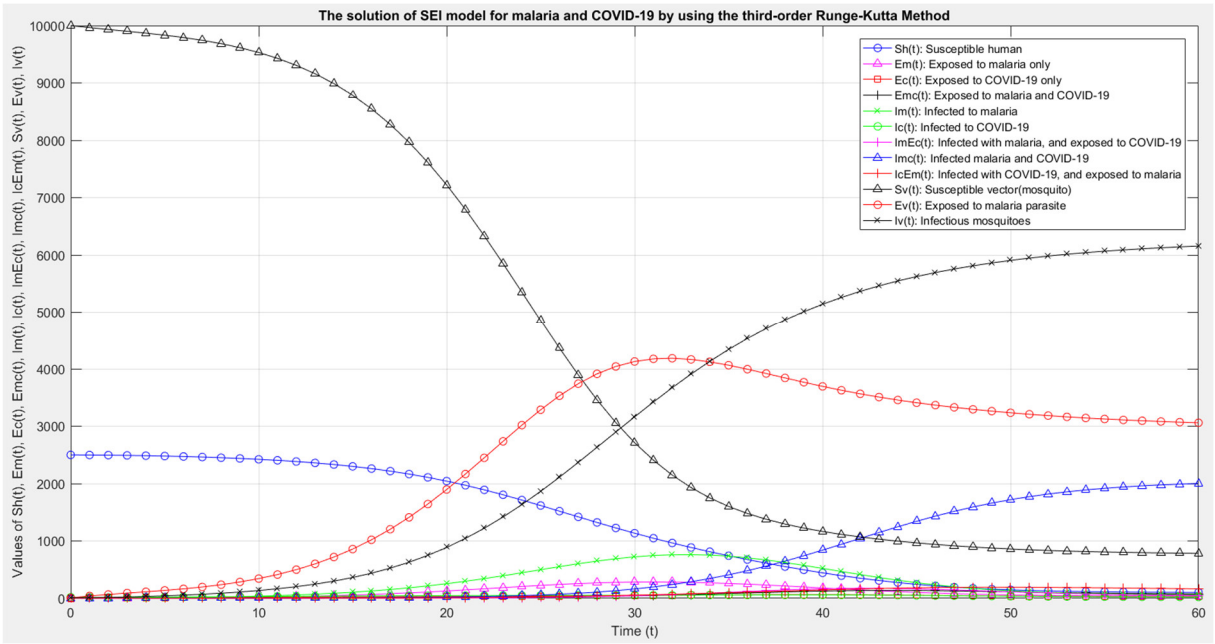

FIGURE 1. Graph of the solution to the spread of malaria and COVID-19 using the third-order Runge-Kutta method with $h = 1$ in the time range [0, 60].

Furthermore, the number of mosquito populations (vectors) in each subpopulation has decreased or increased continuously over time. The number of susceptible mosquitoes, namely S_v, has decreased over time. Then the number of mosquitoes exposed to the malaria parasite, namely E_v, has increased over time. The number of mosquitoes that experienced an increase also occurred in the subpopulation of infectious mosquitoes, namely I_v. However, as time t approaches infinity, the number of mosquitoes will approach equilibrium. In other words, the mosquito population never extinct.

Simulation Results of the Fourth-Order Runge-Kutta Method

Figure 2 shows the results of the co-dynamics of the spread of malaria and COVID-19 with the SEI model using the fourth-order Runge-Kutta method. These results have similarities with the simulation results using the third-order Runge-Kutta method. The patterns of spread and behavior are also the same as those of the third-order Runge-Kutta method.

Method Accuracy Order

The solution patterns of the two methods are the same, as shown from the results of the simulations in Figure 1 and Figure 2. Meanwhile, one of the third-order and the fourth-order Runge-Kutta methods has better order of accuracy. Thus, it is necessary to measure the numerical error and the order of accuracy using the ODE45 algorithm in the MATLAB software for reference solution with 'RelTol' of 2.3×10^{-14} and 'AbsTol' of 1×10^{-15}. This is done because no exact analytical solution has been found for the SEI model in this paper.

To test numerical errors in each subpopulation, we use the absolute error formula. To calculate the order of accuracy for the time steps 1, 0.5, 0.25, 0.125, 0.0625, and 0.03125 we use the error results and the accuracy order formula is [42]

$$R_i = \frac{\log\left(\frac{E_i}{E_{i+1}}\right)}{\log\left(\frac{\Delta x_i}{\Delta x_{i+1}}\right)} \tag{11}$$

Here E_i is the error corresponding to the simulation using independent variable step Δx_i, and E_{i+1} is the error corresponding to the simulation using independent variable step Δx_{i+1}.

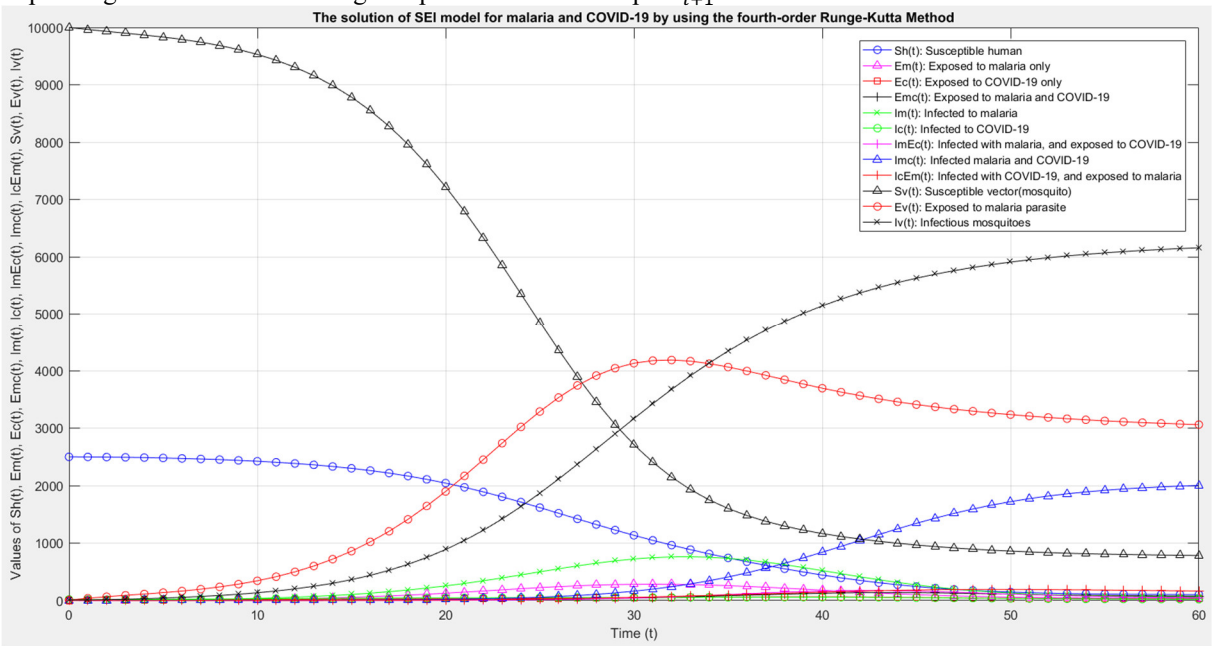

FIGURE 2. Graph of the solution to the spread of malaria and COVID-19 using the fourth-order Runge-Kutta method with $h = 1$ in the time range [0, 60].

TABLE 5. Average error of the third-order Runge-Kutta method

h	S_h	E_m	E_c	E_{mc}	I_m	I_c	I_{mE_c}	I_{mc}	I_{cE_m}	S_v	E_v	I_v
1	14×10^{-2}	8×10^{-2}	4×10^{-2}	3×10^{-2}	15×10^{-2}	2×10^{-2}	5×10^{-2}	19×10^{-2}	3×10^{-2}	58×10^{-2}	48×10^{-2}	52×10^{-2}
0.5	20×10^{-3}	9×10^{-5}	4×10^{-3}	3×10^{-3}	19×10^{-3}	2×10^{-3}	6×10^{-3}	25×10^{-3}	3×10^{-3}	79×10^{-3}	62×10^{-3}	69×10^{-3}
0.25	26×10^{-4}	10×10^{-4}	4×10^{-4}	4×10^{-4}	24×10^{-4}	2×10^{-4}	7×10^{-4}	33×10^{-4}	4×10^{-4}	104×10^{-4}	79×10^{-4}	89×10^{-4}
0.125	34×10^{-5}	12×10^{-5}	5×10^{-5}	5×10^{-5}	30×10^{-5}	3×10^{-5}	9×10^{-5}	41×10^{-5}	5×10^{-5}	133×10^{-5}	100×10^{-5}	114×10^{-5}
0.0625	43×10^{-6}	15×10^{-6}	6×10^{-6}	7×10^{-6}	38×10^{-6}	3×10^{-6}	11×10^{-6}	52×10^{-6}	7×10^{-6}	168×10^{-6}	125×10^{-6}	143×10^{-6}
0.03125	54×10^{-7}	19×10^{-7}	7×10^{-7}	8×10^{-7}	48×10^{-7}	4×10^{-7}	14×10^{-7}	66×10^{-7}	9×10^{-7}	212×10^{-7}	157×10^{-7}	179×10^{-7}

TABLE 6. Average error of the fourth-order Runge-Kutta method

h	S_h	E_m	E_c	E_{mc}	I_m	I_c	I_{mE_c}	I_{mc}	I_{cE_m}	S_v	E_v	I_v
1	104×10^{-4}	186×10^{-4}	103×10^{-4}	31×10^{-4}	163×10^{-4}	77×10^{-4}	25×10^{-4}	49×10^{-4}	12×10^{-4}	463×10^{-4}	336×10^{-4}	135×10^{-4}
0.5	72×10^{-5}	93×10^{-5}	50×10^{-5}	13×10^{-5}	76×10^{-5}	34×10^{-5}	13×10^{-5}	34×10^{-5}	6×10^{-5}	280×10^{-5}	189×10^{-5}	98×10^{-5}
0.25	46×10^{-6}	51×10^{-6}	27×10^{-6}	6×10^{-6}	41×10^{-6}	18×10^{-6}	7×10^{-6}	22×10^{-6}	3×10^{-6}	173×10^{-6}	113×10^{-6}	66×10^{-6}

0.125	30×10^{-7}	30×10^{-7}	16×10^{-7}	3×10^{-7}	24×10^{-7}	10×10^{-7}	4×10^{-7}	14×10^{-7}	2×10^{-7}	108×10^{-7}	69×10^{-7}	42×10^{-7}
0.0625	19×10^{-8}	18×10^{-8}	10×10^{-8}	2×10^{-8}	14×10^{-8}	6×10^{-8}	3×10^{-8}	9×10^{-8}	1×10^{-8}	67×10^{-8}	43×10^{-8}	27×10^{-8}
0.03125	12×10^{-9}	11×10^{-9}	6×10^{-9}	1×10^{-9}	9×10^{-9}	4×10^{-9}	2×10^{-9}	6×10^{-9}	1×10^{-9}	42×10^{-9}	26×10^{-9}	17×10^{-9}

Table 5 and Table 6 show that the average error values in each subpopulation are different for each h. In addition, the average error values between subpopulations using the third-order Runge-Kutta method are larger than those using the fourth-order Runge-Kutta method.

TABLE 7. Accuracy Order of the third-order Runge-Kutta method

h	S_h	E_m	E_c	E_{mc}	I_m	I_c	I_{mE_c}	I_{mc}	I_{cE_m}	S_v	E_v	I_v
1	-	-	-	-	-	-	-	-	-	-	-	-
0.5	2.814	3.167	3.312	3.032	2.963	3.279	3.028	2.922	2.940	2.875	2.956	2.912
0.25	2.918	3.092	3.199	3.015	2.975	3.151	3.010	2.960	2.960	2.926	2.976	2.956
0.125	2.960	3.044	3.106	3.006	2.986	3.073	3.004	2.980	2.980	2.962	2.987	2.978
0.0625	2.980	3.021	3.054	3.003	2.993	3.035	3.002	2.990	2.990	2.981	2.993	2.989
0.03125	2.990	3.010	3.027	3.001	2.996	3.017	3.001	2.995	2.995	2.991	2.997	2.994

TABLE 8. Accuracy Order of the fourth-order Runge-Kutta method

h	S_h	E_m	E_c	E_{mc}	I_m	I_c	I_{mE_c}	I_{mc}	I_{cE_m}	S_v	E_v	I_v
1	-	-	-	-	-	-	-	-	-	-	-	-
0.5	3.856	4.320	4.367	4.596	4.413	4.486	4.280	3.849	4.365	4.047	4.153	3.788
0.25	3.945	4.167	4.190	4.342	4.215	4.256	4.126	3.925	4.152	4.015	4.067	3.903
0.125	3.975	4.086	4.098	4.189	4.111	4.135	4.061	3.963	4.071	4.005	4.032	3.953
0.0625	3.988	4.043	4.050	4.100	4.056	4.069	4.030	3.981	4.034	4.002	4.015	3.977
0.03125	3.994	4.022	4.025	4.052	4.028	4.035	4.015	3.991	4.017	4.001	4.008	3.989

Furthermore, Table 7 and Table 8 show that the accuracy of the third-order Runge-Kutta method is close to a certain value, namely 3, while the accuracy of the fourth-order Runge-Kutta method is close to 4. Then, the order accuracy results confirm that the fourth-order Runge-Kutta method's accuracy is better than the third-order Runge-Kutta method.

CONCLUSIONS

We have solved the SEI model effectively for the co-dynamic problem of the spread of malaria and COVID-19 using the third-, and the fourth-order Runge-Kutta methods. The solution from the simulation results of both methods using the MATLAB software show similarities. Therefore, it is necessary to look for the values of the numerical errors and the order of accuracy of each method to find the difference between the third-order and the fourth-order Runge-Kutta methods. The results obtained from our study confirmed that the fourth-order Runge-Kutta method is indeed more accurate than the third-order Runge-Kutta method in solving the co-dynamics of the spread of malaria and COVID-19 diseases with the SEI model.

ACKNOWLEDGMENTS

The authors thank Sanata Dharma University for the funding support. We are also grateful for the ideas, and the opinions in discussion forums given by one member of the authors' study group, Ms. Dewi Isabella Palma.

REFERENCES

[1] Supranelfy Y, Oktarina R. Gambaran Perilaku Pencegahan Penyakit Malaria di Sumatera Selatan (Analisis Lanjut Riskesdas 2018). *BALABA* 2021; 17: 19–28.
[2] Resmawan. Model Epidemik SEIRS-SEI Penyebaran Penyakit Malaria dengan Vaksinasi dan Pengobatan. *SENAMAS* 2017; 1–3.
[3] Soedarto. *Malaria*. Jakarta: CV Sagung Seto, 2011.
[4] Menkes. Pedoman Tata Laksana Malaria. *http://www.djpp.depkumham.go.id* 2013; 5–61.
[5] PP&PL DJ. *Pedoman Penatalaksanaan Kasus Malaria di Indonesia*. Jakarta, http://www.pediatricfkuns.ac.id/data/ebook/INFEKSI Pedoman_Malaria_di_Indonesia.pdf (2008).
[6] Dimi B, Adam A, Alim A. Prevalensi Malaria Berdasarkan Karakteristik Sosio Demografi. *Jurnal Ilmiah Kesehatan* 2020; 19: 4–9.
[7] Sabilu Y, Irma. Kajian Kasus Malaria Terkonfirmasi Positif Di Sulawesi Tenggara Berdasarkan Variabel Epidemiologi. *Jurnal Farmasi Sains dan Praktis* 2021; 7: 224–232.
[8] Hakim L. Malaria: Epidemiologi dan Diagnosis. *Aspirator* 2017; 3: 107–116.
[9] Ngwa GA, Shu WS. A Mathematical Model for Endemic Malaria with Variable Human and Mosquito Populations. *Mathematical and Computer Modelling* 2000; 32: 747–763.
[10] Nuha RA, Achmad N, Supu N 'Ain. Analisis Model Matematika Penyebaran COVID-19 Dengan Intervensi Vaksinasi dan Pengobatan. *Jurnal Matematika UNAND* 2021; 10: 406–422.
[11] Putra AZ, Abidin SAZ. Application of SEIR Model in COVID-19 and The Effect of Lockdown on Reducing The Number of Active Cases. *Indonesian Journal of Science and Technology* 2020; 5: 185–192.
[12] Li Q, Guan X, Wu P, et al. Early Transmission Dynamics in Wuhan, China, of Novel Coronavirus–Infected Pneumonia. *New England Journal of Medicine* 2020; 382: 1199–1207.
[13] Nurazisah S, Febriawati H, Pratiwi BA, et al. Pengetahuan dan Sikap Berhubungan dengan Risiko Penularan Virus Covid-19 pada Masyarakat di Wilayah Kerja Puskesmas Lingkar Barat Kota Bengkulu. *Jurnal Kesehatan Masyarakat Indonesia* 2021; 16: 160.
[14] Lin Q, Zhao S, Gao D, et al. A conceptual model for the coronavirus disease 2019 (COVID-19) outbreak in Wuhan, China with individual reaction and governmental action. *International Journal of Infectious Diseases* 2020; 93: 211–216.
[15] Chairani I. Dampak Pandemi Covid-19 Dalam Perspektif Gender Di Indonesia. *Jurnal Kependudukan Indonesia* 2020; 2902: 39.
[16] WHO. Transmisi SARS-CoV-2: implikasi terhadap kewaspadaan pencegahan infeksi. 2020; 1–10.
[17] Hastuti N, Djanah SN. Studi Tinjauan Pustaka: Penularan Dan Pencegahan Penyebaran Covid-19. *An-Nadaa: Jurnal Kesehatan Masyarakat* 2020; 7: 70.
[18] Levani Y, Prastya AD, Mawaddatunnadila S. Coronavirus Disease 2019 (COVID-19): Patogenesis, Manifestasi Klinis dan Pilihan Terapi. *Jurnal Kedokteran dan Kesehatan* 2021; 17: 44–57.
[19] Badan Litbangkes P dan P. Ikhtisar Mingguan Covid 19 Di Indonesia. *Pusdatin, Kemenkes* 2021; 1–21.
[20] Putri RN. Indonesia dalam Menghadapi Pandemi Covid-19. *Jurnal Ilmiah Universitas Batanghari Jambi* 2020; 20: 705.
[21] Sinaga LP, Nasution H, Kartika D. Stability Analysis of the Corona Virus (Covid-19) Dynamics SEIR Model in Indonesia. *Journal of Physics: Conference Series* 2021; 1819: 012043.
[22] Hariadi P, Lokida D, Naysilla AM, et al. Coinfection With SARS-CoV-2 and Dengue Virus : A Case Report Highlighting Diagnostic Challenges. *Frontiers in Tropical Diseases* 2022; 3: 801276.
[23] Akil SNH. Penanganan Malaria pada Pandemi COVID-19. *Proceeding Universitas Muhammadiyah Surabaya* 2020; 105–112.
[24] WHO. Tailoring malaria interventions in the COVID-19 response. *Global Malaria Programme* 2020; 34.
[25] Sardar S, Sharma R, Alyamani TYM, et al. COVID-19 and Plasmodium vivax malaria co-infection. *IDCases* 2020; 21: e00879.
[26] Hussein R, Guedes M, Ibraheim N, et al. Impact of COVID-19 and malaria coinfection on clinical outcomes: a retrospective cohort study. *Clinical Microbiology and Infection* 2022; 28: 1152.e1-1152.e6.
[27] Resmawan, Yahya L, Pakaya RS, et al. Analisis Dinamik Model Penyebaran COVID-19 dengan Vaksinasi. *Jambura Journal of Biomathematics* 2022; 3: 29–38.
[28] Osman MA-RE-N, Ebenezer A, Adu IK. A SEIR-SEI Malaria Transmission Model with Optimal Control. *Journal of Advances in Mathematics and Computer Science* 2018; 28: 1–17.
[29] Pramesthi SRPW. Analisis Model SEI Tanpa Vaksinasi Pada Penyebaran Penyakit Tuberculosis (TBC).

Widyaloka 2018; 5: 1–13.
[30] Mutua JM, Wang F Bin, Vaidya NK. Modeling malaria and typhoid fever co-infection dynamics. *Mathematical Biosciences* 2015; 264: 128–144.
[31] Hezam IM, Foul A, Alrasheedi A. A dynamic optimal control model for COVID-19 and cholera co-infection in Yemen. *Advances in Continuous and Discrete Models* 2021; 2021: 108.
[32] Omame A, Rwezaura H, Diagne ML, et al. COVID-19 and dengue co-infection in Brazil: optimal control and cost-effectiveness analysis. *The European Physical Journal Plus* 2021; 136: 1090.
[33] Avusuglo WM, Han Q, Woldegerima WA, et al. COVID-19 and malaria co-infection: do stigmatization and self-medication matter? A mathematical modelling study for Nigeria. *Social Science Research Network* 2022; 4090040.
[34] Wijayanti H, Setyaningsih S, Wati M. Metode Runge Kutta Dalam Penyelesaian Model Radang Akut. *Ekologia* 2011; 11: 46–52.
[35] Chapra SC, Canale RP. *Numerical Methods for Engineers*. New York: McGraw-Hill, 2015.
[36] Tchoumi SY, Diagne ML, Rwezaura H, et al. Malaria and COVID-19 co-dynamics: A mathematical model and optimal control. *Applied Mathematical Modelling* 2021; 99: 294–327.
[37] Triatmodjo B. *Metode Numerik*. Yogyakarta: Beta Offset, 2002.
[38] Mathews JH, Fink KD. *Numerical Methods Using MATLAB.* Fourth Ed. 2004.
[39] Mungkasi S. Variational iteration and successive approximation methods for a SIR epidemic model with constant vaccination strategy. *Applied Mathematical Modelling* 2021; 90: 1–10.
[40] Gusa RF. Penerapan Metode Runge-Kutta Orde 4 dalam Analisis Rangkaian RLC. *Jurnal Ecotipe* 2014; 1: 48–52.
[41] Chapra SC, Canale RP. *Numerical Methods for Engineers,* Eighth Ed. New York, 2021.
[42] Hidayat N, Suhariningsih, Suryanto A, Mungkasi S. The Significance of Spatial Reconstruction in Finite Volume Methods for the Shallow Water Equations. *Applied Mathematical Sciences* 2014; 8: 1411–1420.